Design and Development of a Scaled Test Laboratory for the Study of ABS and other Active Vehicle Systems

by

Amrou Al-Sharif, B.S.

Thesis

Presented to the Faculty of the Graduate School of

The University of Texas at Austin

in Partial Fulfillment

of the Requirements

for the Degree of

Master of Science in Engineering

The University of Texas at Austin

August 2001

Design and Development of a Scaled Test Laboratory for the Study of ABS and other Active Vehicle Systems

Approved by
Dissertation Committee:

Raul G. Longoria, Supervisor

Dedication

This thesis is dedicated to my wife, who put up with me for far too long, and to my mother and late father. I would also like to dedicate this thesis to my two brothers and the rest of my family from Muscat to Houston, including Cairo. Finally, I further dedicate this thesis to the staff members of the Mechanical Engineering department at the University of Texas, especially to those in the machine shop, and to my tutors and mentors who had confidence in my abilities.

Acknowledgements

I would like to acknowledge the following people for contributing to the efforts in developing this thesis:

Gilberto Lopez

Christopher Mackay

Juanmanuel Benavides

David Conrad

Danny Jares

Curtis Johnson

John

Design and Development of a Scaled Test Laboratory for the Study of ABS and other Active Vehicle Systems

Publication No._____

Amrou Adly Al-Sharif, M.S.E

The University of Texas at Austin, 2001

Supervisor: Raul G. Longoria

A $1/5^{th}$ scale vehicle control lab environment was designed and constructed for the testing of maneuvers involving independent front disc brakes with Anti-lock Braking System (ABS) capabilities. An off the shelf radio controlled $1/5^{th}$ scale vehicle was acquired and front disc cable actuated brakes were installed. A test ramp was constructed to accelerate the vehicle and to provide a variable surface test bed for testing of controlled vehicle maneuvers. Optical encoders were installed on the vehicle for acquisition of wheel and vehicle speed. A real-time control engine was programmed to run, control, and acquire data for vehicle control experiments. Experiments were implemented to evaluate the experimental setup using a simple ABS control algorithm. Results show the reliance on the real-time control properties of the RT engine and overall effectiveness of the laboratory for testing of vehicle control algorithms.

Table of Contents

List of Tables

List of Figures

Chapter 1: Introduction

Through out history, moving transports have been fitted with stopping mechanisms to bring the, otherwise, deadly objects to a halt when desired. Stopping safely and quickly applies universally to all vessels. Sailing yachts can heave-to (a maneuver that heads the boat into the wind) and rocket ships can apply reverse thrusters. Ground vehicles, that roll, can be stopped efficiently by limiting the rotation of the wheels via "brakes" and is the most popular method used today. One key issueis that a wheel will lock if the brakes are applied too hard and directional in-stability will follow.

In the beginning of the 20th century, the first anti-lock brake system (ABS) was fitted on a railroad car [1]. However, the motivation in this case was not directional control but to eliminate flat-spots from forming on the steel wheels [1]. It was soon noticed that railcars equipped with ABS stopped in shorter distances than those without ABS. In the 1950's, ABS brakes were installed in airplanes with the first set put on a Boeing B-47, in 1945, to prevent spin outs and tires from blowing[9,1]. Soon after, in the 1960s, high-end automobiles were fitted with rear-only ABS, and the trend exploded in the 1980s. Today, all-wheel ABS can be found on the majority of late model vehicles and even on select motorcycles.

The newest technology incorporates ABS into traction control systems (TCS) and Active Vehicle Handling (AVH). TCS uses ABS to limit wheels spinning under acceleration. AVH can be used as a general term to indicate any added control features that will assist a driver in keeping an otherwise unstable vehicles stable. Currently AVH systems use ABS to help prevent spinouts due to steering maneuvers, through selectively braking the wheels according to variables such as steering angle, vehicle speed, and wheel rotational speed.

Historical as they may seem, anti-lock brake systems do not perform flawlessly. The complexity involved in tire-soil interactions, and the need for on-board estimations

makes ABS algorithms complex, rule based structures. Testing of these algorithms involves overly simplified simulations and expensive, life size, trial and error experimentation for fine-tuning. This thesis contributes to the efforts in providing the foundations for testing ABS algorithms in a laboratory that offers a controllable environment, repeatability, and low cost testing.

Before leading into the focus of this thesis, discussed on page 10, it is first desirable to understand the physics involved with braking. The following sections will hence build the knowledge needed to appreciate the value of this thesis' goals.

TIRE-ROAD DYNAMICS DURING BRAKING

The tire-road dynamics, involved during braking, depend on numerous variables affecting the tire itself as well as the properties of the road surface. The following focuses on the contact patch of the tire and road surface to describe the physics of braking.

Braking Mechanisms

A tire's contact patch is the flat area induced on the tire by the road due to the weight of the vehicle. The width and length of the contact patch depend on the stiffness and size of the tire. Tire stiffness varies according to the construction type, material, and inflation pressures as described in *Tire Technology* by French [2].

During braking, a torque opposing the rotation of the wheel is applied on the tire and braking forces are generated via mechanisms of adhesion and hysterisis as detailed in Figure 1.1 borrowed from *Gillespie's Fundamentals of Vehicle Dynamics* [3]. The adhesive component derives from molecular bonding of the tire to the road and is hence dependent on the surface conditions. For example, water or loose particles in between the tire and road will reduce the adhesion component of the braking force. The hysterisis component stems from the energy dissipation through the hysteric mechanism of the rubber in the tire [4]. The amount of braking force due to hysterisis is controlled via design of the tire's material properties. Increased hysterics in the tire will improve the

braking performance of a tire in wet conditions but compromises the rolling efficiency of the tire. Hysteretic properties contribute to 90-95% of the rolling resistance at speeds of 128-152 km/h (80-95 mph) [4,5], hence careful design parameters must be chosen to achieve optimal performances of tires constructed for specific conditions.

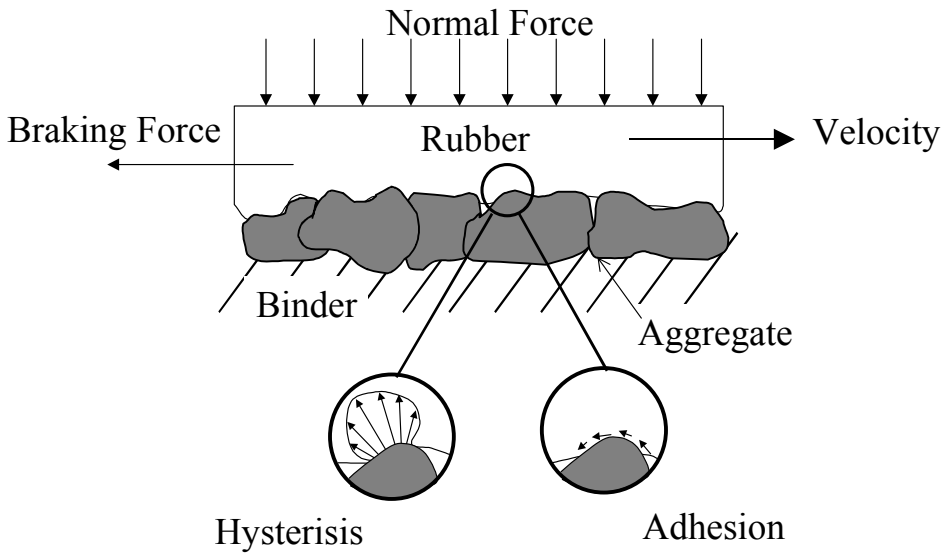

Figure 1.1 Braking Mechanisms [3]

Longitudinal Slip

Longitudinal slip is an important term used to characterize the mechanics of a braked tire and the deformations in the contact patch. As braking torque is applied, the tire elements in the contact patch deform to sustain the braking forces, until finally they begin to slide, starting at the rear [3]. Figure 1.2 shows the relative forces and deformation of the elements in the contact patch. A proportional increase of braking force is observed from the front of the contact patch to the rear. As the braking torque is increased, so do the elemental braking forces until a threshold is reached and the elements, beginning at the rear, start to slide with respect to the road [3]. The combined deformation and sliding of the tire causes the spin velocity of the tire to differ from its equivalent linear velocity referred to as "longitudinal slip" by the Society of Automotive Engineers (SAE) [8].

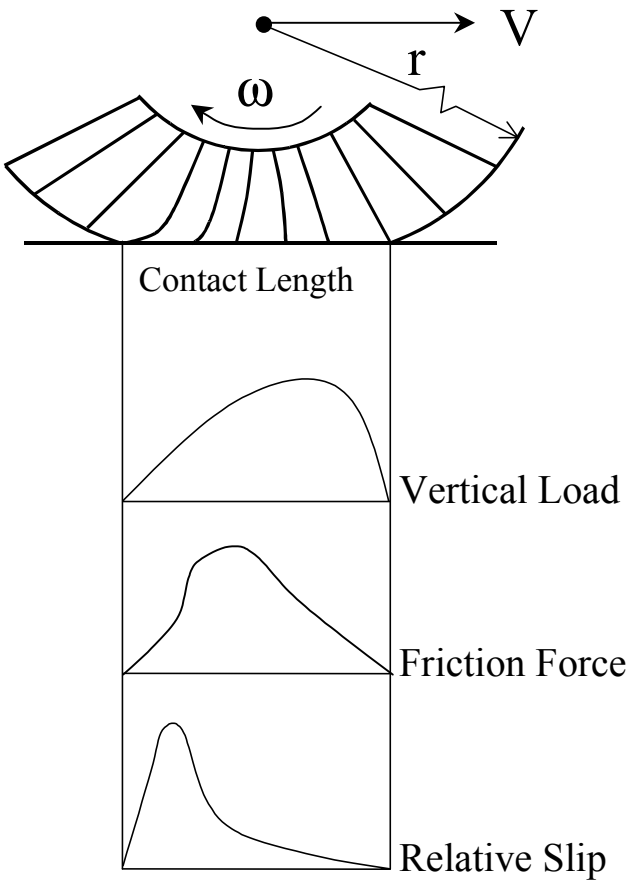

Figure 1.2 Braking deformations in the contact patch [3]

Longitudinal slip is defined by the Society of Automotive Engineers' *Vehicle Dynamics Terminology* [8] as "the ratio of the *longitudinal slip velocity* to the *spin velocity* of the free straight-rolling tire expressed as a percentage" [8]. Longitudinal slip velocity is defined as "the difference between the *spin velocity* of the driven or braked tire and the spin velocity of the straight free-rolling tire." Spin velocity is defined as "the angular velocity of the wheel on which the tire is mounted, about its *spin axis*"; spin axis is defined to be "axis of rotation of the wheel". The spin velocity of the straight, free-rolling, tire can be understood as the equivalent spin velocity if the wheel were perfectly rolling and can be calculated as the ratio of its linear velocity to the non-deformed radius of the tire.

The mechanics are such that the braked or driven wheel will have a spin velocity different from the actual equivalent linear velocity at the center of the tire. In the case of a driven wheel, the spin velocity will be greater than the equivalent spin velocity derived from actual linear velocity of the wheel; and for a braked wheel, the spin velocity will be less than the equivalent spin velocity derived by the actual linear velocity of the wheel. The mathematical equivalences of these descriptions are given by the following equations.

Longitudinal slip velocity can be expressed as

$$i_v = r\varpi - \frac{V}{r} \tag{1}$$

Where i_v is the longitudinal slip velocity, V is the actual linear velocity at the center of the wheel, and r is non-deformed radius of the tire.

Using the definition for longitudinal slip and substituting Eq. (1) for longitudinal slip velocity, the longitudinal slip can be expressed as

$$i = \frac{\left(i_v - \frac{V}{r}\right)}{\left(\frac{V}{r}\right)} \times 100\% = \left(\frac{r\omega}{V} - 1\right) \times 100\% \tag{2}$$

where i is longitudinal slip, and r,ω, and V are as that for Eq. (1).

Using these expressions, -100% longitudinal slip will be observed if the tire is fully locked, 0% longitudinal slip if the tire is free rolling, and if the tire is spinning with no linear velocity then the longitudinal slip approaches infinity. For convenience Eq. (2) is often re-defined as *slip* for a braked wheel and is given as

$$\sigma = \left(1 - \frac{r\varpi}{V}\right) \times 100\%$$

(3)

where σ is slip and r, ω, and V are the same as in Eq. (1). It should be noted that σ is sometimes referred to as "skid" or "spin" however this text refers to it as *slip* in relation to the SAE definition of longitudinal slip [4,9].

For slip calculations using angular velocity rather than longitudinal velocity, Eq. (3) can be re-written as follows:

$$\lambda = \frac{\varpi_{car} - \varpi_{wheel}}{\varpi_{car}} \times 100\%$$

(4)

where λ is wheel slip, ϖ_{car} is the equivalent angular velocity of the vehicle velocity, and ϖ_{wheel} the angular velocity of the braked wheel.

Braking Performance

The tractive force or braking force of a tire on a surface changes non-linearly with slip. A representative curve of this relationship for a tire on a hard surface is shown in Figure 1.3.

Figure 1.3 Variation of Tractive Effort with Slip of a tire

For low slip values, the curve characterizes a linear relationship. This area is representative of the initial flexing and stiffness of the tread on the tire [4]. As slip increases the slope of the curve starts to diminish until a peak is reached that represents the maximum braking or tractive effort. This area and beyond represents the partial sliding of tire elements in the contact patch, starting from the rear as previously mentioned. Beyond the peak point, the tractive effort diminishes. The area beyond the peak is highly unstable as the resultant torque on the tire increases, due to the reduced tractive effort, causing the tire to jerk toward lockup. Experimental studies of pneumatic tires show that the peak usually lies in between 15% and 20% slip [4]. Hence in order to maintain maximum braking it would be desirable to keep the wheel slip at the point of maximum tractive effort. However, due to the instability of this region holding the maximum tractive effort is not easily done manually and needs the aid of an engineered control system.

The next section gives a brief description on how anti-lock brake systems work to maintain the maximum tractive effort or rather the braking coefficient, which is the dimensionless method of describing the overall braking effort and is given by the following equation.

$$\mu = \frac{F_{stopping}}{F_{normal}} \tag{5}$$

where μ is the braking coefficient, F_{normal} is the normal force of the vehicle and $F_{stopping}$ is the stopping force on the vehicle. This method is of describing the braking efficiency works well for use in comparing results for various vehicles, especially when the stopping efficiency is measured in *g*s. For example, a car that has a maximum braking acceleration of 0.7g can be said to have a maximum braking coefficient of 0.7. Of course one must assume that the braking acceleration was given for a level run.

ABS CONTROL

The typical components to an ABS system, shown in Figure 1.4 Typical ABS System, are the Electronic Control Unit, Hydraulic Control Unit, wheel speed sensors, and braking device, which may be a disc brake or drum brake. The HCU actuates the brakes by increasing the hydraulic pressure or bypassing the pedal force to reduce the braking power. The ECU monitors the wheel speed to signal the HCU when to apply and release the brakes.

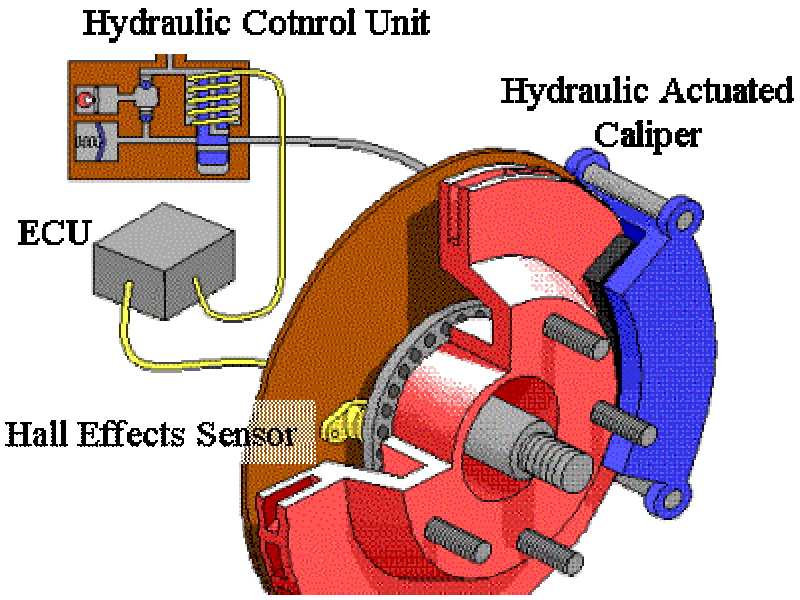

Figure 1.4 Typical ABS System [6]

Recall that maximum traction resides in between 15%-20% slip. In all ABS systems the goal is to prevent the tire from locking and to keep the wheel slip in the region of maximum braking effort. Figure 1.1, burrowed form Gillespie [3], shows that operation cycle of an ABS system. Regularly, as the brakes are applied the wheel slip increases and the wheel slows proportionally (point 1). Once the peak is reached (point 2) the braking coefficient reduces causing the torque opposing the braking torque to diminish, and the wheel uncontrollably heads toward lock up (point 3). In an ABS system, the ECU intervenes at point 2 and cycles the brakes on and off to keep the wheel

slip between point 1 and point 3, ideally at point 2. The apparent cycling frequency is around 20Hz for production vehicles [7,3].

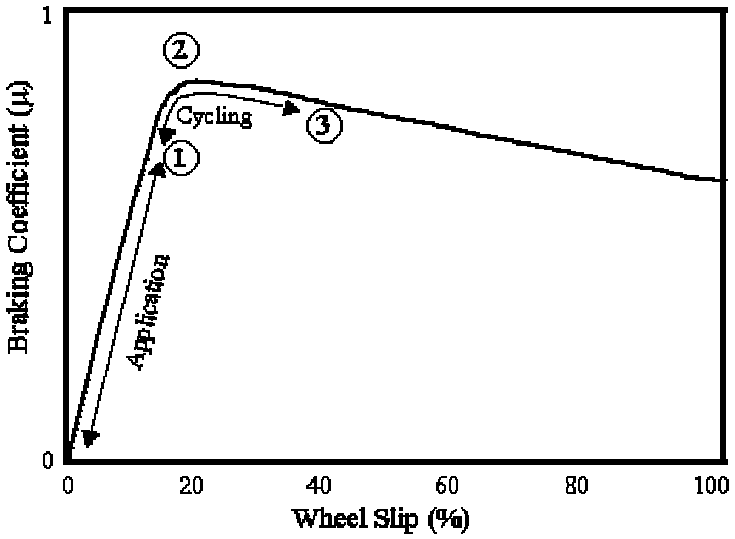

Figure 1.5 ABS Operating Cycle

The task of keeping the wheels operating around the point of maximum braking coefficient is complicated by the ever changing μ-λ curve due to vehicle speed, tire, and road changes. Figure 1.6 adopted from Athan, [15], shows a few profiles due to changes in terrain only.

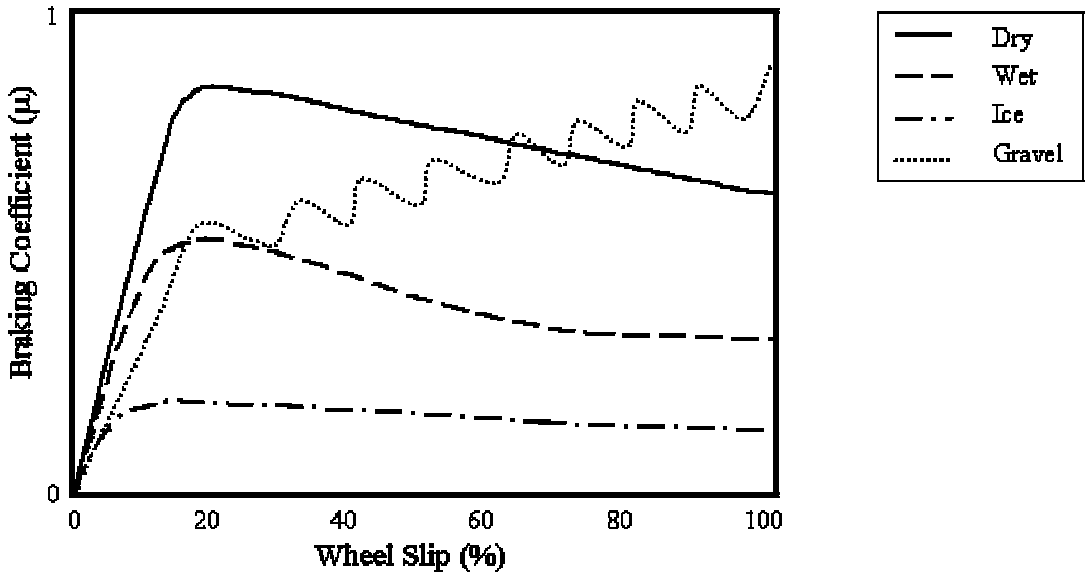

Figure 1.6 Braking Coefficient Curves for Various Surfaces

In order to accommodate the enormous range of operating conditions, complex rule based control systems are employed. Such systems may come in the form of fuzzy, sliding mode, or state space control schemes [13,14,15]. These systems typically use several hundred rules [9]. The rules stored in look-up tables are mostly based on experimental trials completed at the test track [15,7]. Furthermore, due to the fixed structure of the control strategy, the algorithms are tuned down to accommodate for extreme conditions and as consequence non-optimal braking performance is imposed for regular driving conditions. To complicate matters further, key variables such as vehicle speed is not easily measured accurately and must be estimated. In some cases wheel deceleration, instead of wheel slip, is measured to check for impending lock-up. Of course, this method requires system knowledge ahead of time. For example, 1g could be used as the deceleration conditional value as the mechanics, of passenger car vehicles, show 0.8g as the maximum deceleration limit [9].

THESIS FOCUS

Conventional methods of testing algorithms include repeated simulations and track trials. Track trials are expensive, requiring trained drivers and are subject to weather conditions. Using an ABS test laboratory for validation of control algorithms can reduce the amount of Track Trials needed. Furthermore, careful design of the laboratory can allow for future accommodation of active vehicle handling control systems such as steer by wire. This thesis outlines the implementation of such a laboratory with validation based strictly on straight line ABS braking. The laboratory was oriented around a $1/5^{th}$ scale model vehicle fitted with ABS. The goal of this thesis is to show that scaled vehicle handling testing has promise through validation of straight line ABS braking.

REAL –TIME CONTROL

The need to understand the concepts of real-time control is necessary to successfully implementing ABS algorithms, as one of the largest problems with developing robust ABS lies in the real-time estimation of the μ-λ curves [7]. The definition of a real-time system, as is ABS, is labeled by Lawrence as "a system whose temporal performance (response time, data-acquisition period, etc) is of critical importance to the industrial systems to which it is connected" [17]. For ABS, the ECU must acquire the wheel speeds, decide on the appropriate measures to take, and signal the HCU fast enough, otherwise a wheel may lockup. This definition also relates to a system that may require holding the temperature of a 50-gallon water tank. In this case the controller may only need to take temperature measurements every 5 minutes or so to be considered a real-time system.Lawrence gives the design process of a real-time control system in reference [17].

Chapter 2: Laboratory Design

Three different concepts for the proposed laboratory were considered. The first concept consists of a controlled motor spinning a rotor braked by a caliper. Through simulation of various terrain, the motor is controlled to simulate the torques and speeds that ABS sees during a straight line braking maneuver, hence creating a virtual vehicle passing over virtual terrain. Independently controlled, the brake system uses speed sensors and the brake caliper to bring the virtual vehicle to a complete stop. The second and third concepts use a physical, scaled vehicle model with on-board sensors and actuated brakes running over real terrain, which could be varied by simply changing the surface texture. The difference between the second and third conceptsis that the second is constrained to a track where else the third concept is free to steer.

Outlined below are few of the advantages and disadvantages associated with each concept, which were taken into consideration when picking the preferred concept for the final setup.

Concept One

Low cost and a short implementation time are the biggest advantages for the first concept. Only four items would need to be purchased and one fixture built to hold the motor, rotor, caliper, and modulation device to drive the caliper. Measurement of rotor velocity could easily be made available from the motor data or external RPM sensing through the use of hall effects sensors or optical encoders. Furthermore, supporting work on the use of electrical brake calipers and similar test setups for manufactured systems could support the efforts undertaken [].

Disadvantages include the heavy computing and modeling required to accurately simulate a virtual vehicle reducing the possibilities of having a realistic real-time experiment setup. Vehicle and terrain simulations make simplifications in the models for

feasibility and solvability. These simplifications would reduce the advantages to using the laboratory as a verification tool for new software algorithms. Finally this setup would not be useful as visualization tool for teaching purposes and or demonstrations.

Concept Two

The advantage to having an actual vehicle eliminates the need to create a virtual environment and allows the capture of complex physical phenomena. This also opens the possibilities of testing performance of real-time control engines Also, by confining the vehicle to longitudinal motion reduces complications in producing repeatable runs and allows for a less complex vehicle, i.e. steering mechanisms are not required.

The disadvantages, other than actually having to build the setup hence cost and time, is the limitation to longitudinal studies only. Granted that straight line braking algorithms need further study, more complex maneuvers involved in active vehicle handling include steering, would not be achievable with such a setup.

Concept Three

The third concept was to use a scaled vehicle accelerated down a ramp onto a surface for testing. The advantage of this setup is that it allows for all the dynamics involved in real maneuvers and so provide a stepping stone for the testing of new algorithms and control techniques that have been developed through simulation. The biggest reward of this setup is that it could significantly cut the costs and time involved with testing braking algorithms on life size vehicles.

The biggest disadvantage to this setup is the complex undertaking of acquiring and preparing a scaled vehicle with the adequate hardware to implement ABS. Such a vehicle would require steering, suspension, and braking capabilities thus increasing the complexity and cost of the setup. Furthermore, the ability to steer will require extra care in the experiment setup in order to ensure repeatability.

Concept Choice

Though each concept has its advantages and disadvantages the advantages of concept 3 promised for a more flexible platform for vehicle controls testing and hence was more appealing than concept 1 or 2. Furthermore, the use of an off the shelf vehicle would eliminate the need to build a scaled vehicle. It was therefore decided that concept 3 was the ideal choice to develop into a laboratory for the study of ABS and was designed, built and named Vehicle Controls Lab (VCL).

EXPERIMENTAL SETUP

VCL is divided into three major components: the test track, vehicle, and real-time (RT) engine. The basic experimental procedure involves pulling the car up the ramp, releasing, and then implementing a vehicle maneuver. Figure 2.1 shows the test track and vehicle.

Figure 2.1 Test Track and Vehicle

VEHICLE

The design goal was to implement ABS brakes on a scaled vehicle in order to test barking algorithms and real-time control techniques. Furthermore, keeping the ABS control system analogous to those commercially available was desired. This need was most closely met by an off the shelf $1/5^{th}$ scale vehicle. The $1/5^{th}$ scale vehicle is a radio control (RC) car made by FG Modellsport (FGM), a model car manufacturer in Germany. The models made by FGM resemble various production vehicles from VW Beetles to Formula 1 racecars. FGM's vehicle lineup was chosen as they also produce key accessories such as disc brakes and various wheel and tire designs. Furthermore, the vehicle's steering and suspension systems are fully adjustable. These are useful traits if any future studies require changes in tire tread and suspension parameters. The particular model chosen was a Porsche GT2 due to its relatively short wheelbase, allowing for the construction of a shorter ramp. The illustration below shows the Porsche GT2 as advertised by FGM

Figure 2.2 FG Modellsport Porsche GT2

Two types of brake systems were available from FGM, a hydraulic brake system and a cable actuated brake system. Both types of systems use one power source to drive both the left and right brakes. The two systems are shown in the illustrations below.

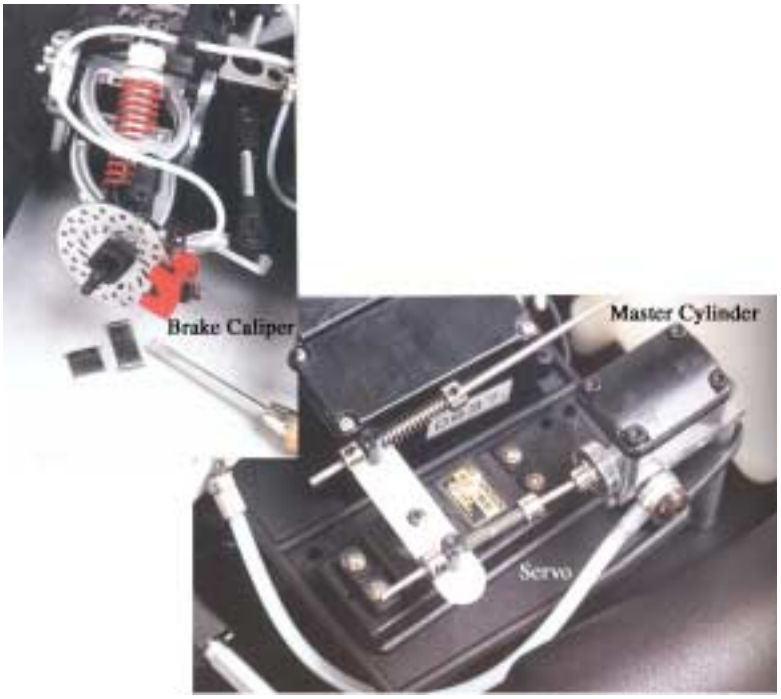

Figure 2.3 FGM Hydraulic Brake System

Figure 2.4 FGM Cable Actuated Brakes (highlighted for viewing)

Both brake systems only actuate the outside brake pad and incorporate a floating rotor that pushes against a stationary inner brake pad. Details on the workings of the calipers

are described in Chapter 3: Modeling and Simulation. Of the two systems, the cable-actuated brake system was used, as it was readily available without a wait period of three months.

For independent control of the front disc brakes, modifications were made to the original braking system. The modifications involved the design and construction of the Servos Holder and two Cable Guides. The Servos Holder simple holds the servos in place and the Cable Guide guides the brake cable to the appropriate servo. The modification is highlighted in the illustration below. Engineering drawings can be found in Appendix A.

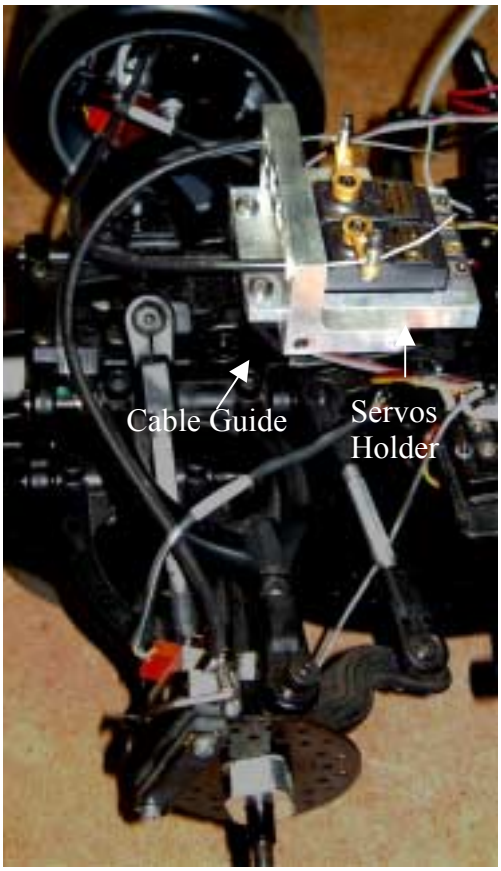

Figure 2.5 Modified Brake System Setup

Powering the brake cables are two modified Futaba S9402 servos. The servos are specified to operate at 4.5 volts and provide a maximum outout troque of 112 oz-in. The maximum rotation is 0.09s/60° or the equivalent of 11.63 rad/s (111 RPM). An input

pulse train signal of 50Hz is read by the servo to determine angular position. The position of the servo output shaft is proportional to the duty cycle of the signal. Duty cycle is defined, as the proportion of the amount of time the signal is high to the period of the signal, as illustrated in the figure bellow.

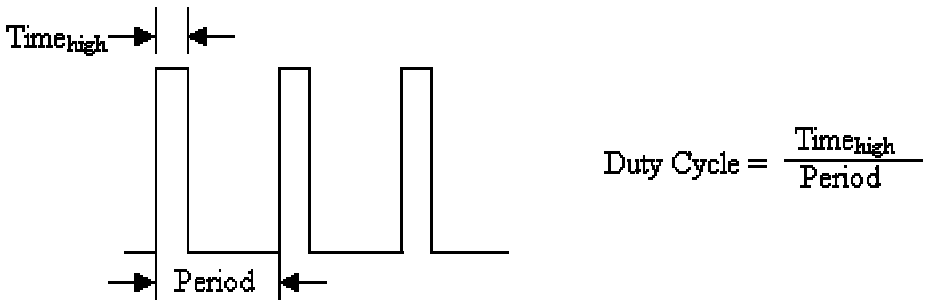

Figure 2.6 Duty Cycle Measurement

The maximum rotation is approximately 260° and the working duty cycle ranges in between 0.87 to 0.95 for the servo.

To make the control of the brake system as analogous as possible to that of an actual brake system, the servos were modified to be used as regular geared motors. Braking force would hence be controlled by voltage, analogous to fluid pressure control driving the baking force in hydraulic systems [10].

For wheel and vehicle speed acquisition, two encoders were attached to each of the front wheel's rotating spindle and a third to the rear differential's source gear. Optical encoders were picked over other sensors for their high resolution in a relatively small package. The encoders used have 1024 counts per revolution (CPR) code wheels and HEDS modules distributed by U.S. Digital. . The encoders are designed such that the slotted area of the code wheel passes between a light emiting diode (LED) and four photo diodes. The bars and slots in the code wheel hence interrupt the light. The photo diodes are placed such that one pair is exposed to the light when the other experiences a dark

period. Signal processing circuitry, built into the encoder, process these signals into two channels, A and B, which are 90 degrees out of phase [16]. Either one of the channels can be used to detect frequency, while both in conjunction can be used to detect rotational direction. Since only shaft frequency was desired, only channel A was needed. The shaft frequency is then simply the proportion of the signal frequency to the number of slots in the encoder or

$$f_{shaft} = \frac{f_{signal}}{N} \tag{6}$$

where f_{shaft} is the shaft frequency, f_{signal} is the signal frequency and N is the CPR of the code wheel.

Also added to the vehicle is a quick release mechanism actuated by a Hi-Tec servo, similar to the Futaba servos used for braking. The quick release mechanism was designed and manufactured in house and attached to the rear of the vehicle. The purpose of the Quick Release is to release the car from the Return Cable, remotely, before a run. Figure 2.7 below shows the Quick Release Mechanism in the locked and release positions.

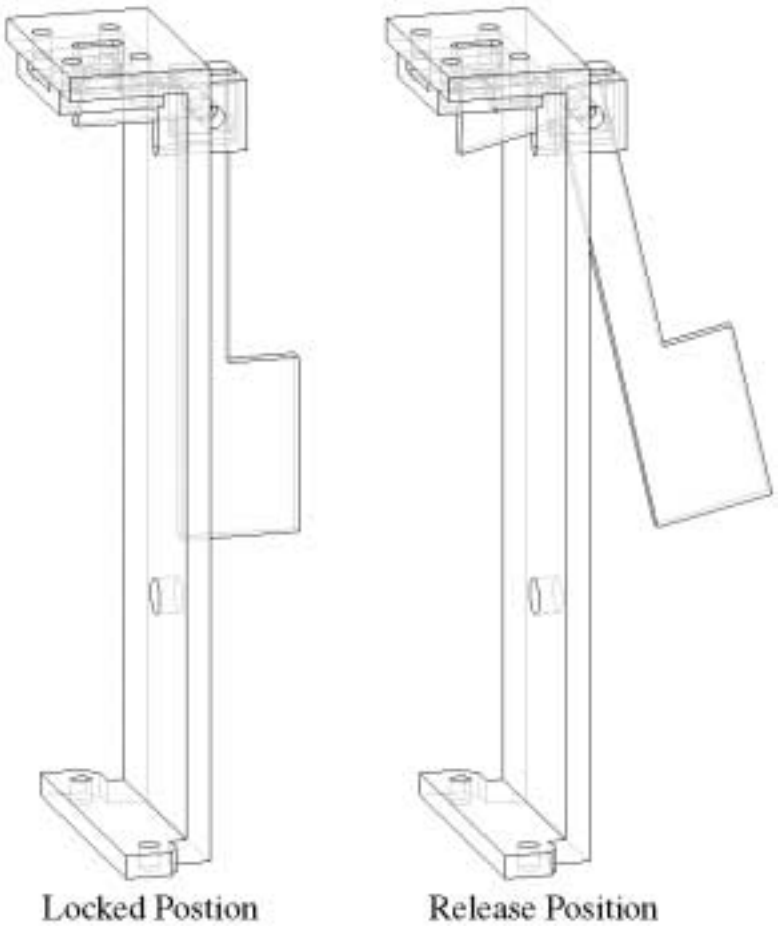

Figure 2.7 Quick Release Mechanism in Locked and Release Postion

A Futaba Digital Proportional Radio Control System is used to remotely steer the vehicle and activate the brake. The system comes in two parts, a handheld controller and a receiver. The hand held controller interfaces with the user for control of steering via a steering wheel and braking via a trigger (Figure 2.8). The signals are transmitted by means of FM to a receiver. Directly plugged into the receiver are two steering servos, coupled to work together. The trigger signal is extracted from the receiver and processed to determine when the user would like to brake.

Figure 2.8 Futaba Digital Proportional Radio Controller

Onboard the vehicle is an in house designed and manufactured Signal and Power Transfer Box (SPTB). The SPTB was designed to simplify and tidy up the power/signal harness used to power the vehicle and communicate with the RT engine. Shown in Figure 2.9, the SPTB measures 4.5 by 7 inches and has three toggle switches, 4 LEDS, a J-45 (Ethernet socket), and leads to the three encoders, release servo, two identical 7.2V battery packs, and one 6Vbattery pack. The toggle switches turn on the steering, brake, and encoder power. The J-45 connection is used for the attachment of an umbilical cord coming from the RT engines data acquisition cards (DAQ). The LEDs serve to indicate when the steering, front brake, right brake, and encoders are powered. The 7.2V batteries are used to power all the servos while the 6V battery pack is used to power the encoders. When the brake switch is off, the right brake LED also serves to indicate when the SPTB is connected to the RT engine.

Figure 2.9 Plan View of SPTB

Eight signals are handled by the SPTB of which four are directed from the vehicle to the RT engine, termed outgoing signals, and three come from the RT engine, termed incoming, to control onboard actuation. The eighth signal is the ground from the RT engine. The outgoing signals consist of the differential, left wheel, and right wheel encoder signals, and the brake signal from the receiver. The three incoming signals are used to control the release servo and the front left and right brake motors. The latter two signals are the only analogue signals communicated and are amplified by an APEX PA26 amplifier wired for unity gain to directly drive the brake motors. All of the signals pass through the J-45 jack. A schematic of the wiring and electronics embedded in the SPTB is shown in Figure 2.10.

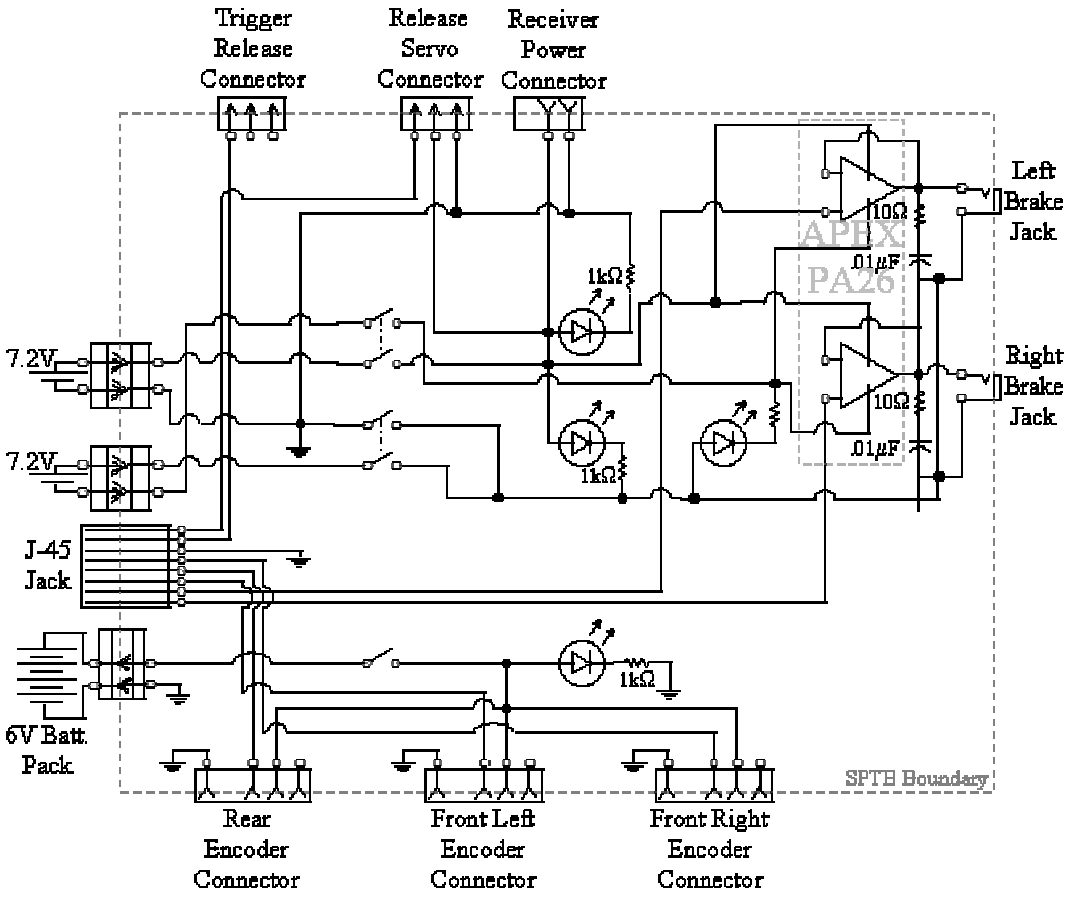

Figure 2.10 SPTB Schematic

TEST TRACK

The test track is divided in two sections, the acceleration portion and test surface portion. The acceleration portion is made of an 80 degree steep ramp and a transition 12ft. in diameter that mates with a horizontal test surface. A variable speed 1/15 hp winch is attached to the top of the acceleration portion to pull up the vehicle. The RT engine, via a servo controls, the speed of the winch. The winch can be run in three modes: Forward, Reverse and Brake. Typically only Reverse is used to pull up the test vehicle to any

desired height less than 8 feet above the surface of the test section. The test surface is removable and can be altered for different terrain..

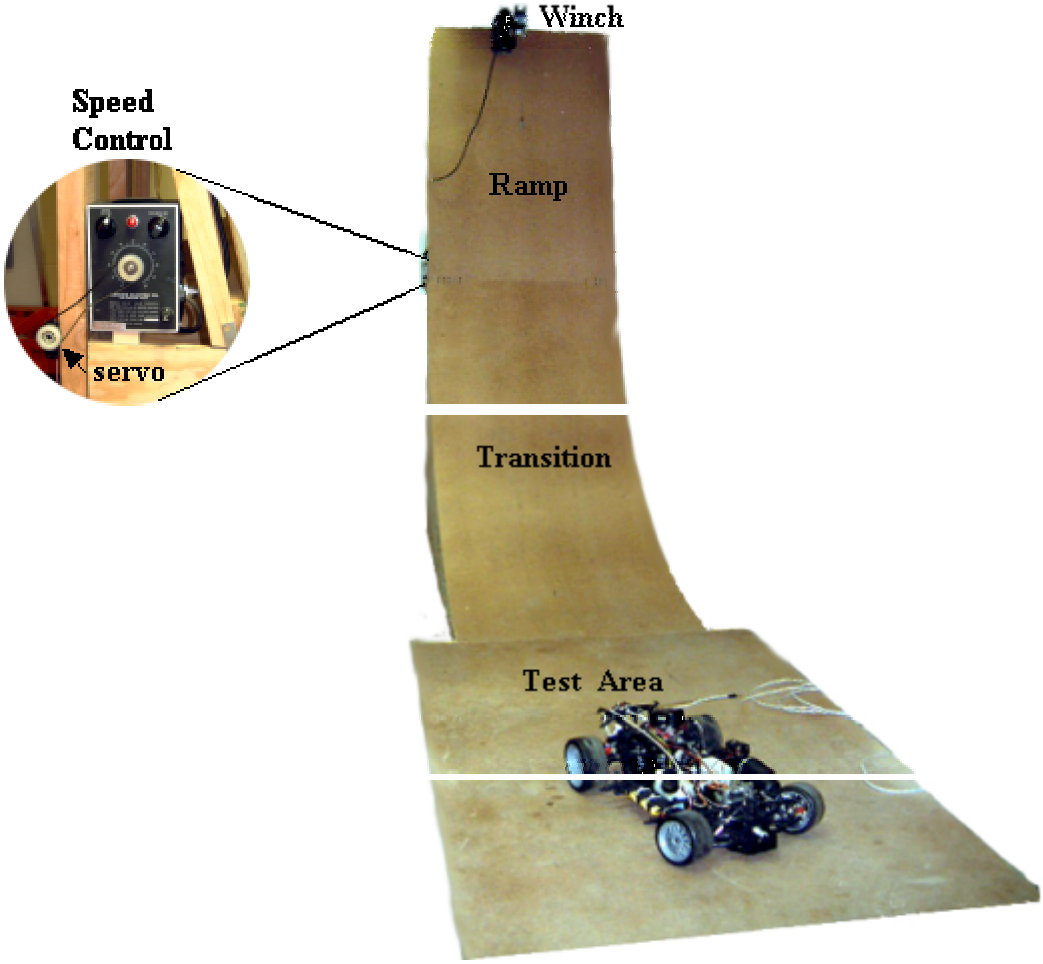

Figure 2.11 Test Track Components

REAL TIME ENGINE

The Real-Time Engine's job is two fold, first it acts as the ECU for the ABS brakes system, and secondly it is responsible for running the experiments and collecting and handling data for analysis.

Physically, the RT engine is the combination of National Instrument's controller PXI-8156B running LabVIEW Real-Time , a NI 6070E Multifunction Input/Output DAQ

card, and a NI 6602 Timing Input/Output DAQ card. All three are plugged into a National Instruments PXI chassis. Programming and communication of the RT engine is done on a host computer, a desktop computer, via an Ethernet or network connection. Figure 2.12 below shows the RT engine with its three main components, and Figure 2.13 shows setup of the RT engine and host computer in the lab. The Virtual Instrument (VI) running on the RT engine is programmed to solely control the ABS system and gather data during a brake run, and is in continues communication with the host computer in between the runs. This allows the use of the host computer to remotely control the winch and to check the on board sensors and actuators. Further discussion on the way RT engine is programmed to run is described in chapter 4.

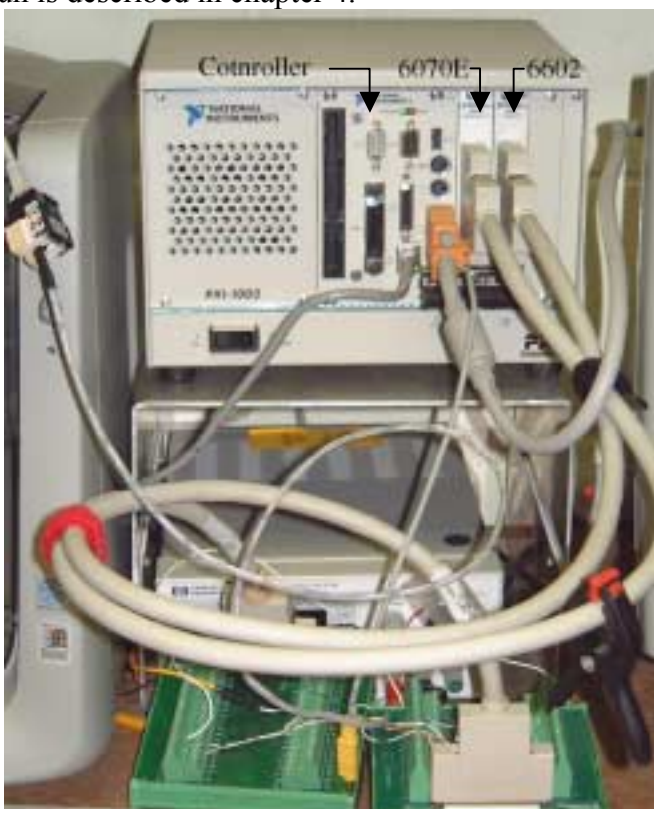

Figure 2.12 RT Engine and Components

Figure 2.13 Host and RT Engine Setup

SIGNALS AND ABS ALGORITHM

In order to simulate a basic ABS controller, the RT Engine reads the TTL signals from each encoder, determines the appropriate braking force and sends that information to the SPTB as analogue signals. This is done by first converting TTL signals into wheel and car speeds to calculate the wheel slip, for each wheel, using (3). Next, depending on the condition correlating to each tire's wheel slip value, an analogue signal representing the braking force to each wheel is sent the SPTB. Currently the logic used to determine the braking force is a simple check to see if the wheel slip lies in the "sweet spot" of the tire-road μ-λ curve, described in Chapter One. The curve was estimated using published data for a $1/15^{th}$ scale model vehicle and is further explained later on in Chapter 3. The initial looped algorithm used by the RT Engine to simulate the ABS controller was as follows:

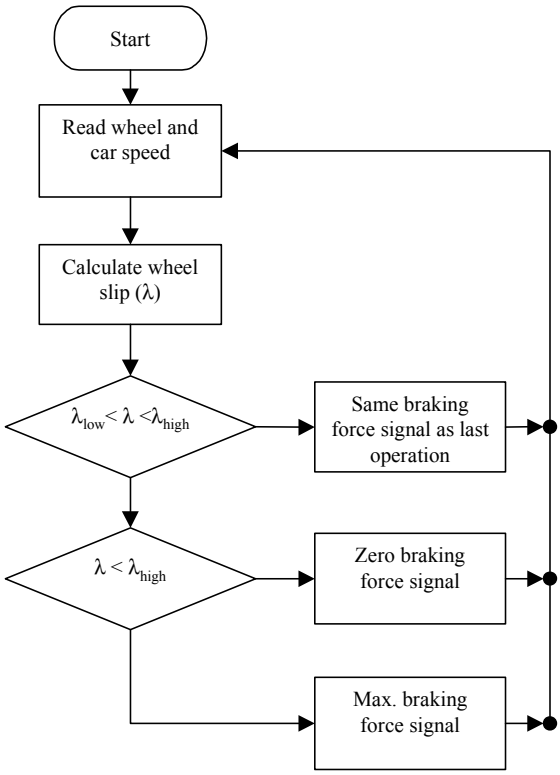

Figure 2.14 ABS Controller Algorithm

In order to repeat this procedure with the minimum loop rate, a buffered counter acquisition technique was used. This technique eliminates the necessary requirement of initializing each counter, used for the acquisition of the encoder and brake signals, for every reading. Furthermore, this technique also takes advantage of data acquisition's Direct Memory Access capabilities that helps acquire data faster. Chapter 4 gives a more detailed explanation on how this is accomplished and the benefits gained.

The analogue signals sent to the SPTB represent voltages of how much braking force to apply. In the case of hard braking with ABS, the signals represent either maximum braking or zero braking. The analogue signal is then amplified by the SPTB as described earlier. The amplified signal directly drives the motor of the appropriate brake servo. The maximum and zero braking voltage signals are 5V and -0.6V respectively.

The negative voltage is used to help the cable disc brake system overcome the servo gearbox friction.

Chapter 3: Model and Simulation

A simulation was created to determine if a realistic ABS braking sequence could be implemented on the $1/5^{th}$ scale RC car equipped with the cable actuated disc brakes powered by the modified servomotors. Since off the shelf components were chosen to reduce the costs and time to implementation, a simple simulation was needed to deduce capabilities of these components. The focus of the simulation was on the capabilities of the servo and the manufacture's cable-caliper design. The results of the simulation showed promising characteristics of the brake system and justified the use of the modified Futaba servo as an actuation brake source.

To simplify the simulation the full model, termed the ABS Model was broken into three components: the vehicle-road model, the braking system model, and the ABS logic model. The simulation was created in Simulink® by MathWorks™.

The Bond graph method was used as the preferred method of modeling as the bond graphs can be graphically read and present a physical likeliness to the actual system. *Physical modeling* by Rosenberg and Karnopp [10. Rosenberg, R., Karnopp, D., *Introduction to Physical System Dynamics*. New York, McGraw-Hill Inc. 1983 is a good introduction to modeling with bond graphs.

The surface chosen for the simulation brake tests was a low μ surface, more specifically the smooth side of Hardboard a panel made of consolidated wood fibers through heat and pressure in a hot press [7]. The low μ surface reduces the amount of braking force required to lock the wheels making it easier to reach the unstable region in the μ-slip curve, hence magnifying the advantages of an ABS system.

The figures below show the lab test setup, part of the car, and brake system. Note that for the actual braking setup each caliper has its own servo, thus there are two front brake servos, one for each wheel as described in the previous chapter.

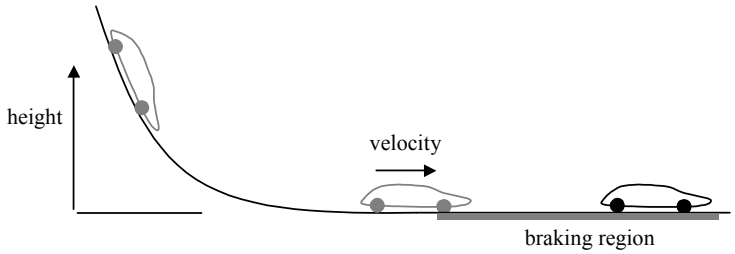

Figure 3.1 Brake Test Setup

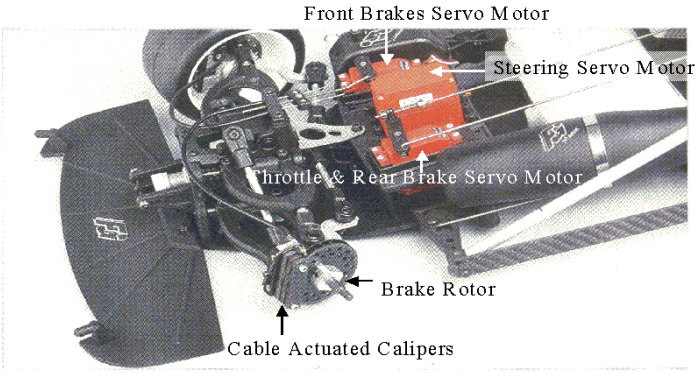

Figure 3.2 Vehicle Brake Setup

SERVO MOTOR MODIFICATION

There were changes made to the servo control so that the braking torque at the wheel could be directly controlled rather than the angular position of the servo arm. Simply disconnecting the control system of the servo, and directly feeding the actual motor a voltage achieved the desired result and essentially changes the servo into a DC motor driven gearbox.

ABS VEHICLE MODEL

The ABS model consists of three main components, the Car Road system, the Brake System, and the ABS Control System. Each system is modeled after actual physical characteristics, except for the control system, simply a collection of logical operations.

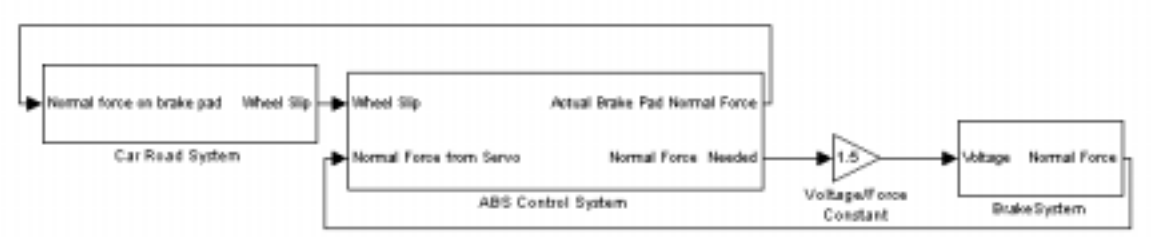

Figure 3.3 Complete Simulink Model

Brake System Model

The Brake System comprises of a *Brake Servo*, *Cable*, *Return Spring*, *Rod*, *Cam*, *Rotor* (disc), and two *Brake Pads*. The figure below shows the components of the Brake System and how they relate to one another.

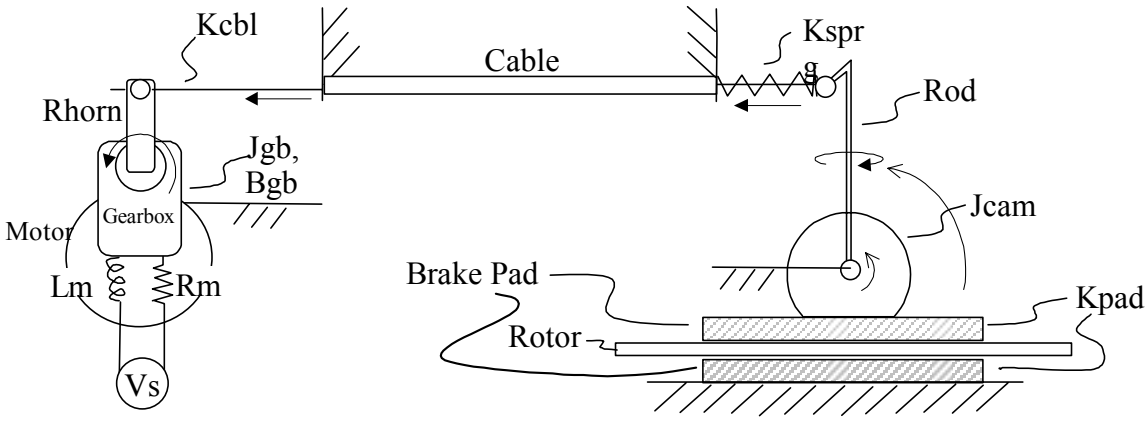

Figure 3.4 Diagram of Brake System Elements

The *Brake Servo*, *Rod* and *Cam* components were modeled in detail in order to accurately capture the response characteristics crucial to pulsation attribute of ABS braking. Damping in the Brake Pads and Cable was neglected. Other parameters were measured or calculated and are given in the Appendix. Motor parameters were derived from manufacturer specifications. Bond graph models of these sub components are given in the following sections.

Brake Servo

The modifications to the Futaba servo make the brake servo a regular DC *Motor* attached to a *Gearbox*. Powering the *Motor* is the voltage source *Vs*. *Vs* is a controlled voltage sent by the ABS controller. The electric circuitry of the motor was modeled as an inductor with inductance *Lm*, resistor with resistance *Rm*, and gyrator in series. The gyrator couples the electric and mechanical aspects through the gyration constant, sometimes called the motor constant, *rm*. The gearbox was modeled as linear mechanical transformer with inertia *Jgb* and a damping resistance of *Bgb*. The schematic below shows elemental representation of the motor and gearbox with their respective parameters.

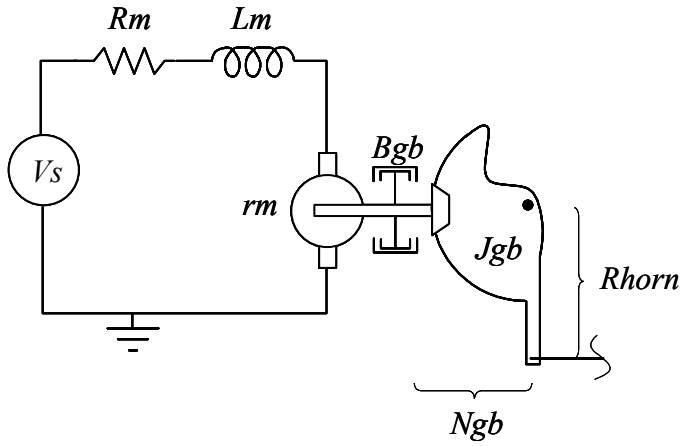

Figure 3.5 Motor and Gearbox Schematic

The actual servo gearbox consists of many gears with the servo horn attached to the output gear. The overall gear ratio, *Ngb*, includes the radius of the horn

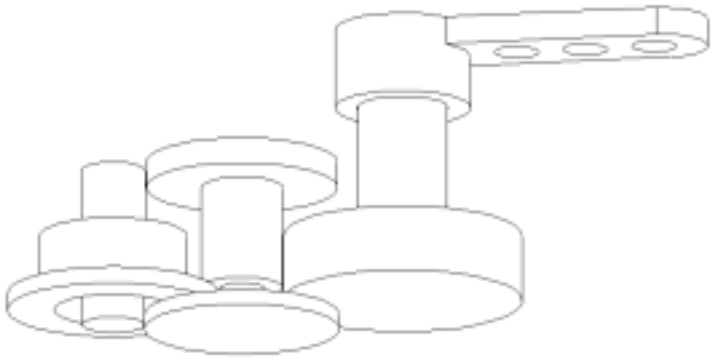

Figure 3.6 Actual Gear Box and Servo Horn

The bond graph of the motor and gearbox is given below.

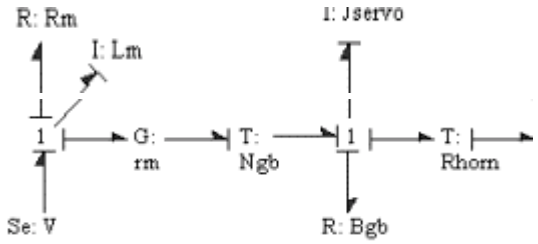

Figure 3.7 Bond Graph of Modified Brake Servo

Rod and Cam

The element labeled *Rod*, in Figure 3.5, is a 2.2 millimeter steel rod bent at approximately 90 degrees. The *Rod* has a ring on the end of the shorter arm of which is pulled on by the brake cable and pushed on by a return spring. The longer arm is fixed perpendicularly to the *Cam* with the shorter arm in parallel with the *Cam*'s face. During braking, the *Rod* undergoes relatively high bending and torsion strains playing a large role in the brake system's characteristics. For this reason the *Rod* was modeled in detail. The figure below shows the *Rod* element's geometry, its stiffness parameters *Krodbeam*

and *Krodtor*, and relation to the *Cam*. It should be noted that the *Rod* is fixed relative to the *Cam*.

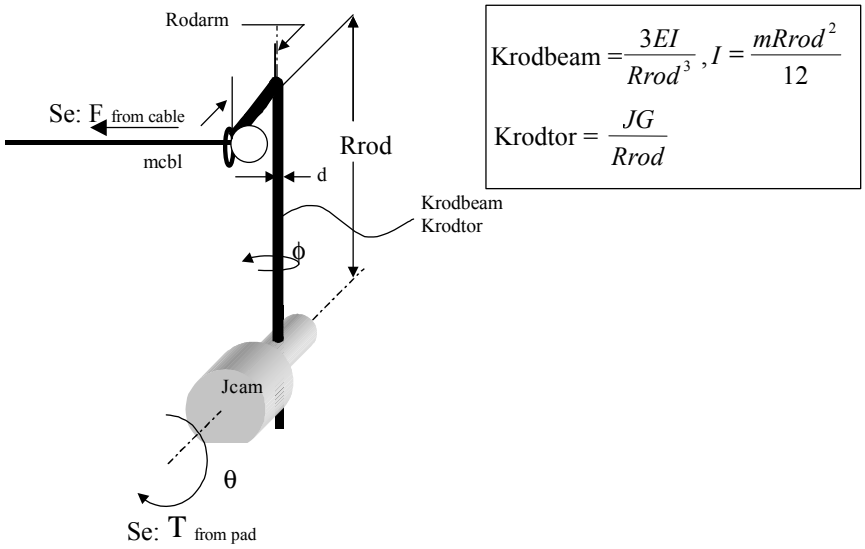

Figure 3.8 Detailed Diagram of *Rod*

As the cable pulls on the *Rod*, the *Rod* undergoes torsion and bending in the longer section of the *Rod* of length *Rrod*. Compliance in the shorter section of the *Rod* is neglected due to the short length of the arm. The representation of the *Rod*, in bond graph form, reveals the dependency of the flow, causing bending, on the torsion angle. The dependency is modeled as a modulated transformer and is shown below in Figure 3.9.

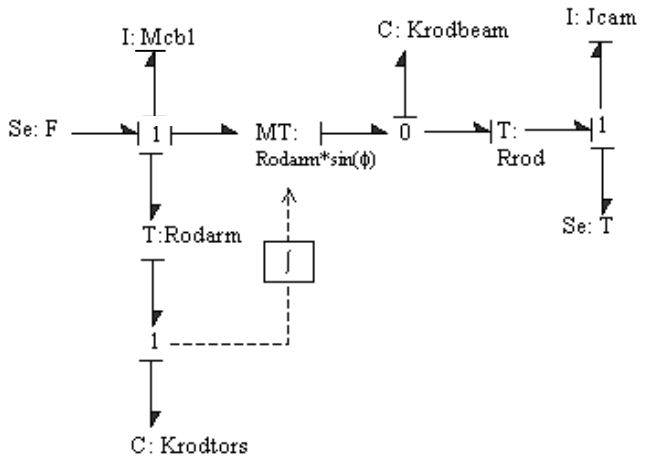

Figure 3.9 Rod and Cam Bond Graph

Complete Brake System

During braking, the edge of the flat on the *Cam* pushes the *Brake Pad* against a floating *Rotor*. The moving *Brake Pad* forces the *Rotor* against a stationary brake pad causing the rotor to be squeezed. This action is modeled as modulated transformer where the rotation angle of the *Cam*, θ, modulates the moment arm. Combining the bond graphs shown in Figure 3.7 and Figure 3.9, adding the *Cable* and *Return Spring*, and including the *Cam* action and *Brake Pads* completes the bond graph of the Brake System, shown below in Figure 3.10.

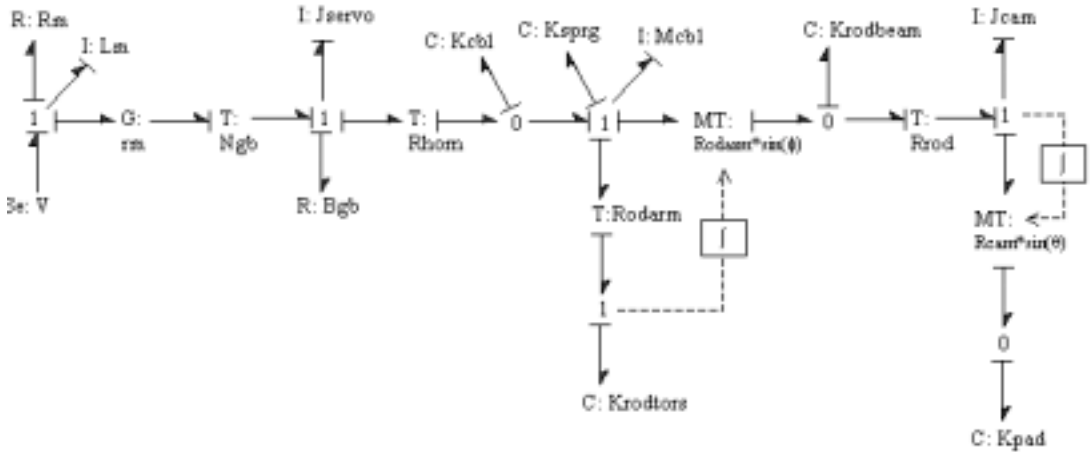

Figure 3.10 Bond Graph of Brake System

Car-Road System Model

The Car Road System was broken up into three basic components, the *Wheel*, the *Road* and a *Tire-Road* interface as a medium to transfer the torque from one to the other. For simplification, the road was modeled as a wheel with inertia, *Jcar*, in contact with the braked wheel of inertia *Jwheel*. Jcar is equivalent to that of the car, as the tire sees it. Since the simulation was of one front wheel, the mass used to calculate the inertia of the car was ¼ of the total car mass. Jcar was hence calculated as

$$Jcar = Mcar \times Rwheel^2 \tag{7}$$

Where Jcar is the inertia of the road as the tire sees it, Mcar is ¼ the weight of the car, and Rwheel is the radius of the wheel.

A input torque, τ_{brake}, to the wheel represents the braking torque given from the Brake System. The tire-road interface transmits the torque between the Road and the Wheel according to the tire-road constitutive relationship described below.

Figure 3.11 below shows a diagram of the simplified Car Road System.

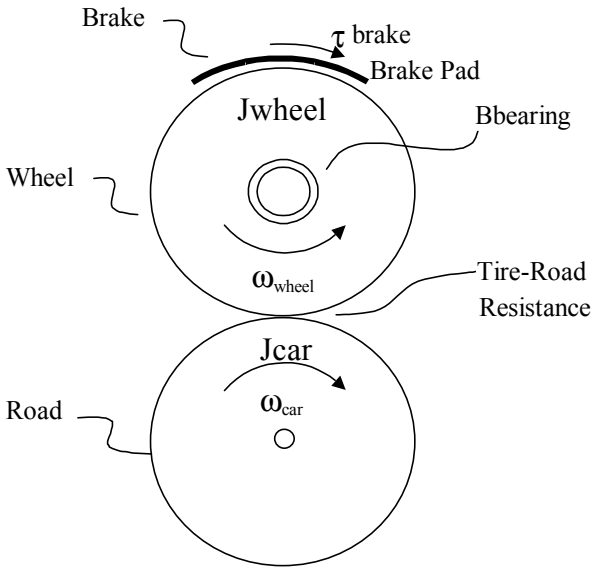

Figure 3.11 Simple Vehicle Model

The tire-road interface was modeled as a resistive element dependent on the wheel slip λ. The wheel slip is determined by the following equation

$$\lambda = \frac{\varpi_{car} - \varpi_{wheel}}{\varpi_{car}} \tag{8}$$

The constitutive relationship between λ and the resultant tire-road coefficient of friction, μ, was created by first matching the profile of a μ-λ curve generated from experimental results done for the 1/5th scale modeled vehicle described earlier and in reference [12], then roughly scaling the curve to represent the surface and tire used. Appendix A contains more information on how this was done.

The braking torque is governed by the normal force of the Brake Pads on the Rotor and the coefficient of friction between the Brake Pads and the Rotor. The static and kinetic coefficient o friction, μ_s and μ_k respectively, for the Rotor–Brake Pad interface was measured and look up table was created with the following relation

$$\tau_{brake} = N \times \begin{cases} \mu_s, \omega = 0 \\ \mu_k, \omega \geq 0 \end{cases} \tag{9}$$

where τ_{brake} is the braking torque, N is the normal force on the Rotor, ω is the angular velocity of the wheel, μ_s is the static coefficient of friction, and μ_k is the kinetic coefficient of friction. Brake fade and other changes due to temperature and wear was not taken into consideration. Finally, the conditions set in equation (9 were offset by a negligible amount to allow for a continuity. The values used are given in appendix A.

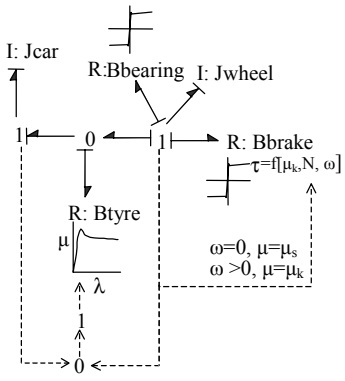

Figure 3.12 Vehicle-Road Bond Graph

Control System Model

As mentioned before the control system is a collection of logic statements that gives a required brake force given the wheel slip, λ. The logic is such that the appropriate brake signal is given to keep the wheel slip is within the region of the μ-λ curve that generates the maximum adhesion, the "sweet spot" region. The logic is such that:

If the wheel slip falls below a certain predetermined value, λ_{low}, the control system sends a signal to the brake system to apply the maximum brake force.

If the wheel slip goes above a predetermined vale, λ_{high}, it sends a signal for minimum brake force.

If the wheel slip is in the sweet spot region, the current signal is maintained to hold the current brake force setting.

Figure 3.13 below shows the relative relationships of λ_{low}, λ_{high} and the sweet spot region and Figure 3.14 shows the logic implemented in a Simulink model.

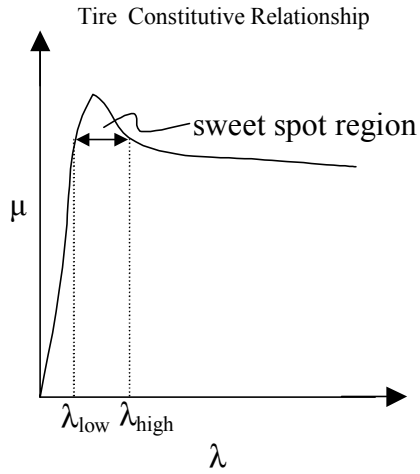

Figure 3.13 Sweet Spot Region

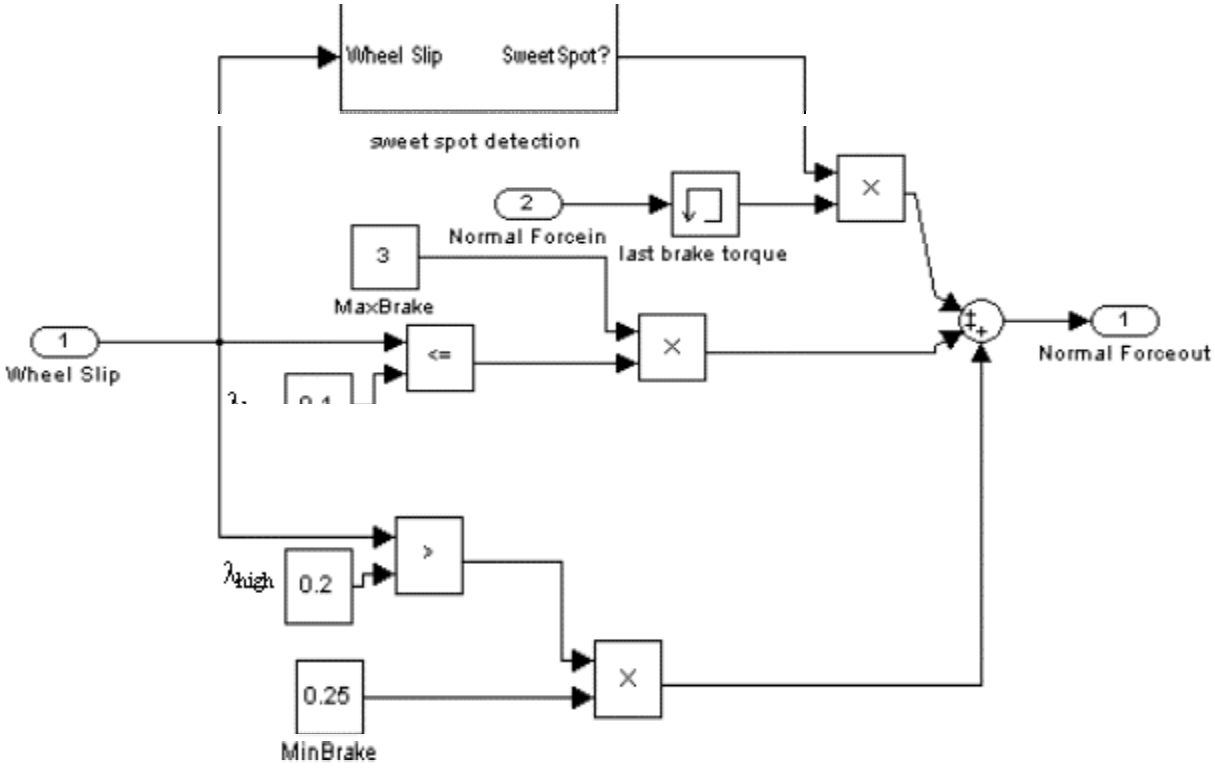

Figure 3.14 Simulink Model of Logic Used by ABS Controller

The Max Brake or Min Brake signal represents the required normal force at the caliper for maximum and minimal braking respectively. The actual 1/5th scale vehicle brakes had a slight braking torque even when the brakes were completely released and therefore a

small normal force was specified for the Min Brake signal. The signal is then passed through a gain that gives the voltage required by the servo to produce the needed normal force at the brake pad.

Complete Model

The complete bond graph for all three systems is shown in the Figure 3.15 below, note that the Brake System and Car Road System are only coupled via information signals, which represents the ABS Control System. Note that the brake signal to the servo is amplified to give the maximum available voltage when Max Brake is required. The maximum voltage was set at 4 volts, which required a gain of 1.5 for the brake signal as shown in Figure 3.3.

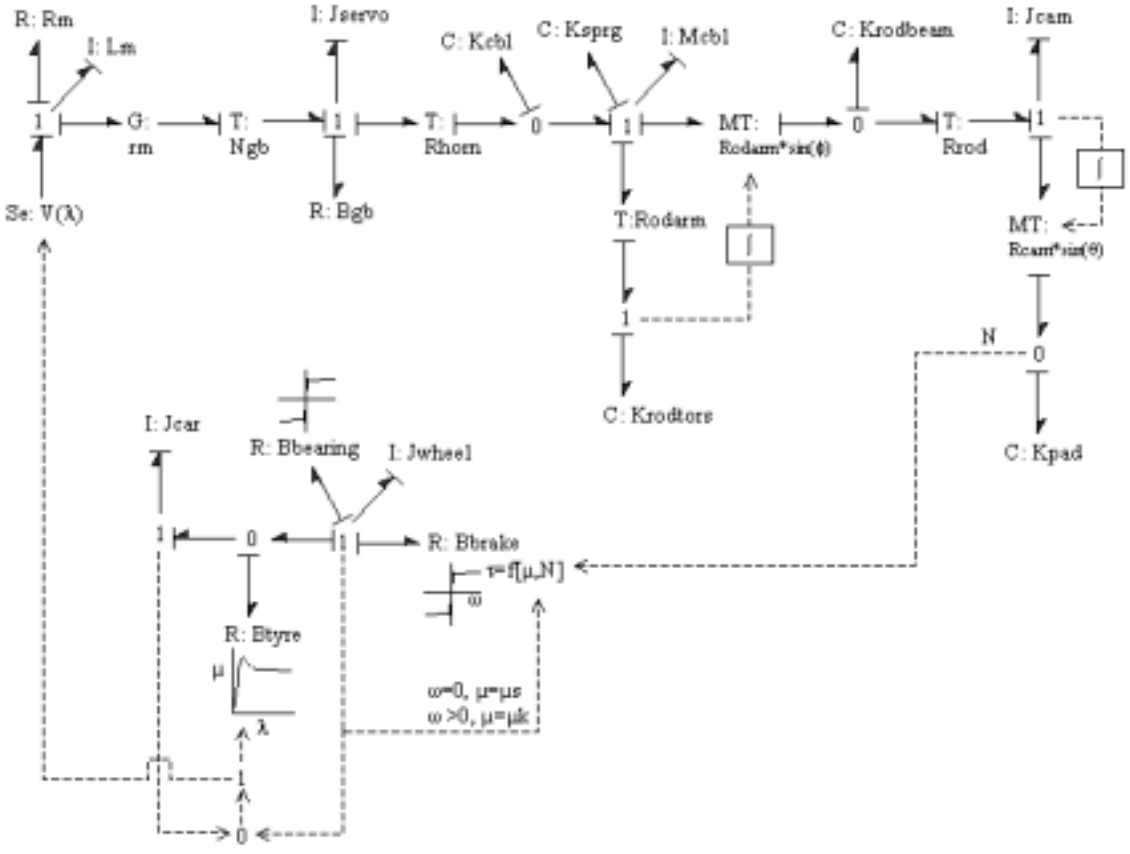

Figure 3.15 Complete ABS System Model

SIMULATION AND RESULTS

Each system model mentioned was created and implemented in Simulink. A variable step stiff type solver, ode15s in Simulink, was used to perform the integration, as the whole model was an eleven order relatively stiff model.

Simulation Setup

Four simulations were run for two separate cases. The first case began the simulation with a high initial vehicle speed of 35 mph. The second began with a lower initial speed comparable to releasing the vehicle 60 vertical inches up the ramp. For each case was run twice, with the ABS control system turned on, and again with the ABS system turned off. In all runs, a panic stop was represented, meaning that without ABS the wheel was locked throughout the braking procedure.

Simulation Results

Two graphs, for each case, were generated to analyze the data. The graphs can be seein in Figure 3.16 below. On the first graph, of each case, the velocity of the wheel speed, vehicle speed, wheel slip, and brake torque was plotted. On the second graph, the stopping distances for a run with and without ABS were plotted. In both cases, the data showed that the brake system was able to respond fast enough to stop the car faster with ABS then without ABS.

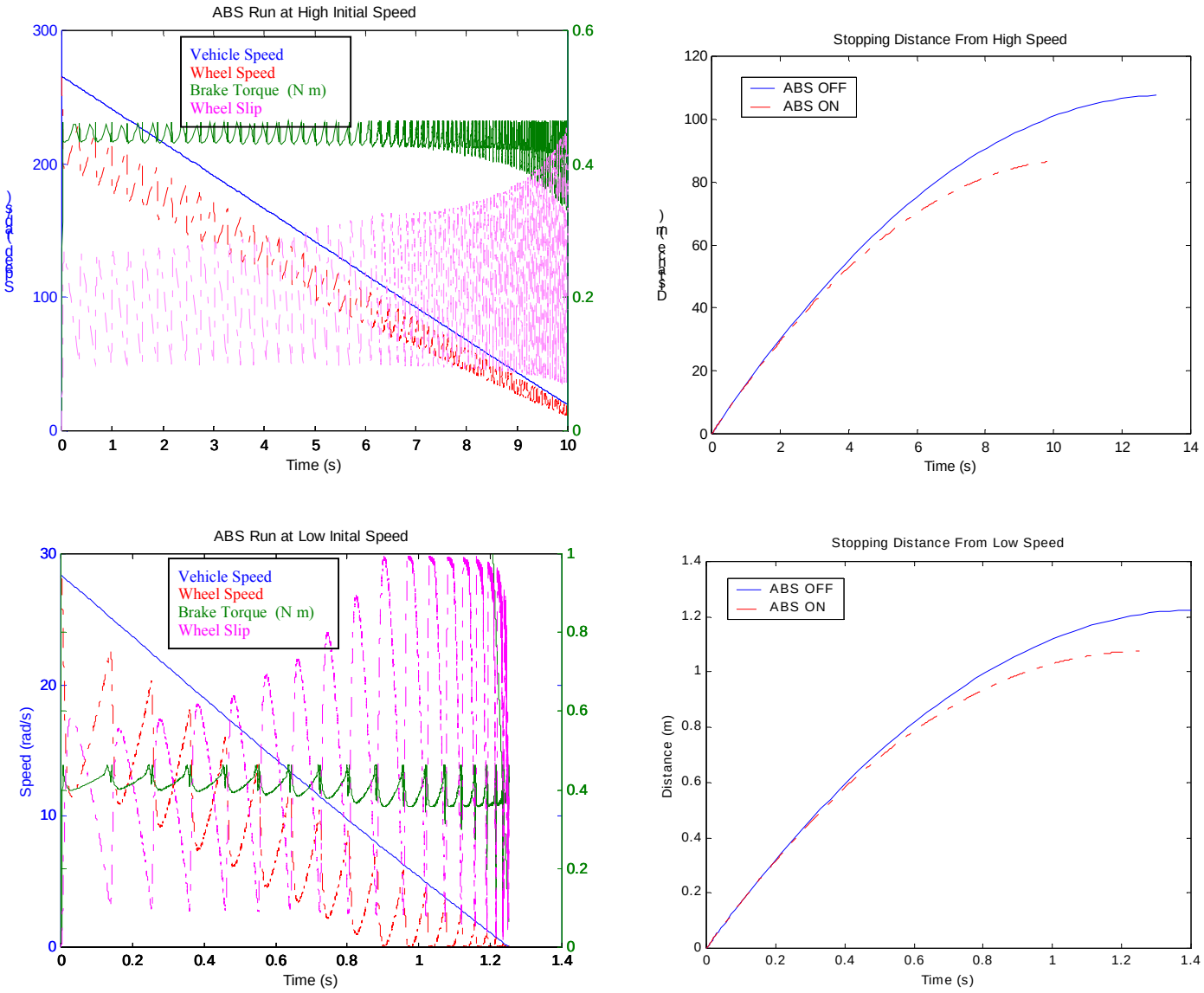

Figure 3.16 Vehicle Response Simulation Responses

The limiting factor to the success of an implemented ABS system is the braking system. Another graph was made to specifically analyze the simulated brake system's response to the high frequency ABS control switching. Figure 3.17 Brake System Responsebelow shows that the normal force is indeed being changed fast enough to keep the wheel from locking. However, the wheel slip fluctuates between 0.1 and 0.55 and is weighted such that the average wheel slip is greater than 0.25, outside the sweet spot

area. The ABS performance the is therefore not ideal. The same figure also reveals that the magnitude of wheel acceleration was greater when the brake was applied versus when it was released. This is consistent with the brake dynamics discussed earlier. Furthermore, this knowledge could be used to adjust the primitive ABS control logic used in the simulation; a good example of the required fine-tuning and high costs involved with ABS.

Finally, a simulation was run to test the response of the brake system to a 6 volt step input. The graph shows the result of the brake system test and demonstrates a first order type response with less than 10ms time constant. Acknowledging that variables such as slack in the system were not taken into consideration, the response is faster that of the wheel heading toward lockup or free spin.

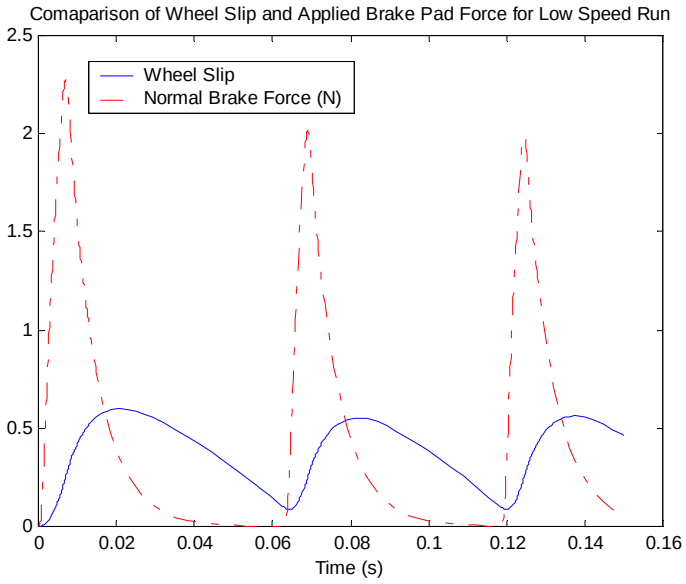

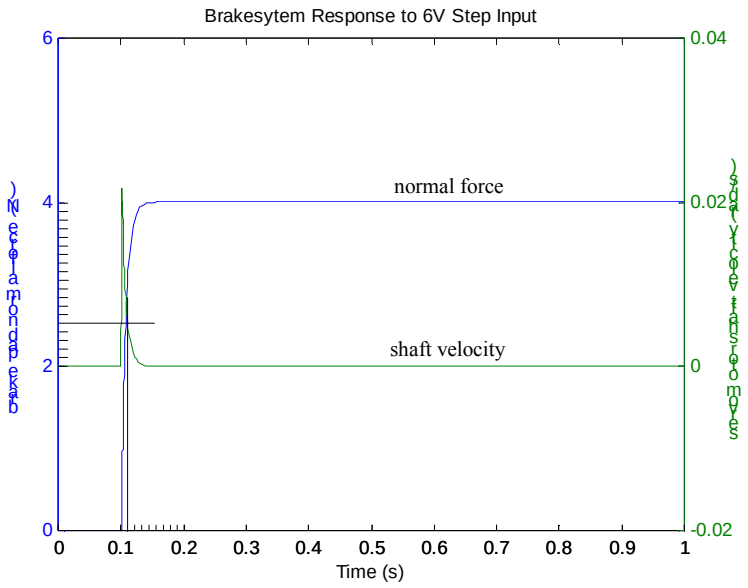

Figure 3.17 Brake System Response

Overall, the simulation data showed that the servo and brake-system used are adequate to implement the real-time control of an ABS system on the 1/5th scale model vehicle. Furthermore, given that the tire-road interaction is fairly represented, the low initial vehicle speeds used in the labs are adequate to demonstrate the advantages of ABS.

Chapter 4: Real-Time System Design

As described earlier, requirements of the RT System included representing the ECU as well as provide a complete test and measurement system. LabVIEW Real-Time was chosen to develop the real-time software as it fully supported the accompanying hardware mentioned in Chapter 2. The following describes the methods used to accomplish the tasks of the real-time system.

SETUP

In order to understand the methods used to accomplish the required loop rates to achieve ABS, with the FGM braking system, a basic explanation on the workings of the real-time system is warranted.

LabVIEW Real-Time

LabVIEW Real-Time (RT) was chosen as the programming language since it provided a real-time OS and seamlessly supported the data acquisition hardware donated by National Instruments for this study. LabVIEW, on LabVIEW RT adds on as a module, is a software programming tool for developing programs in G, a graphical programming language. Programs written in LabVIEW are called Virtual Instruments (VIs), and generally have two parts, the Diagram and Front Panel. The Diagram is used to draw the program, in a block diagram manner, where functions are represented as icons with the data traveling along "wires" connecting the functions together. The Front Panel is used to enter and view data to and from a VI using graphical controls and indicators. One of the advantages that LabVIEW has over other software programming applications, besides

allowing G based programming, is the vast libraries of sub VI's, functions, that facilitate data acquisition, signal processing, and transmission tasks. LabVIEW also has numerous built in features that allow the use of graphical controls and indicators for creating graphical user interfaces (GUIs) for VIs. In creating the VI used for the laboratory, features such as sliders, buttons and dials were used to give the program a user friendly, control panel feel. LabVIEW RT , the specific software used for the laboratory, is almost identical to LabVIEW with extra features for Real-Time applications, such as running the VIs on a headless, embedded controller with a real-time operating system. It is the author's experience that developing the VI's in LabVIEW RT had no difference from developing them in LabVIEW, as far as actual programming was concerned. However, to achieve more deterministic results, a better understanding of LabVIEW was needed such as understanding how LabVIEW handled memory allocations.

Host and Target Communication

As previously shown, the real-time system consists of the Host and Target system. Development of the VI is done on the Host computer. Once completed, it is downloaded to the Target, the RT Engine, for implementation. The Target operating system incorporates the bare necessities needed to support the VI and hardware. Waiving the necessary interrupts and updates used in regular operating systems saves the Target valuable processing time and allows for a more robust platform. For example, the Target does not support a mouse nor graphics hence the operating system need not check for mouse input or update the display.

However, this feature forces the need for communication between the Host and Target if there is to be interaction with the user. There are two methods the user can utilize to interact with the RT engine. The first uses a feature of LabVIEW RT that establishes a thread between the host and target to RT engine, on the host, the target's VI's front panel and block diagram. The second method involves developing code that allows a User Interface VI to communicate with the VI running on the RT engine. The main advantage of the first method is that no extra code was required and disadvantage was that all the actual data processing and management would be occurring on the RT engine, which would consume precious processing time. The advantage of the second method is that with a separate VI running on the host PC, the host PC's processor could be used to handle all of the data management, processing and analysis needs. The disadvantage was that this method would require more development time as communication between the RT engine and the host would have to be programmed manually.

In general, communication with the Host will slow down the potential real-time loop rates as communication introduces specific protocols, such as TCP/IP, to be implemented. Furthermore, such communication requires non-deterministic handshaking, which further cripples real-time capabilities. Special attention is therefore given to heavy hardware real-time demands and is implemented differently from those that require real-time communication with the user.

Real-Time System Functional Requirements

Before designing the Laboratory VI a list of functional requirements for the Real-Time system was generated. These requirements were then categorized in two sets, those that required user interaction and those that needed to be accomplished in real-time. Figure 4.1 below, shows the arrangement of the functional requirements and their placement in the categorized sets in a Venn diagram format.

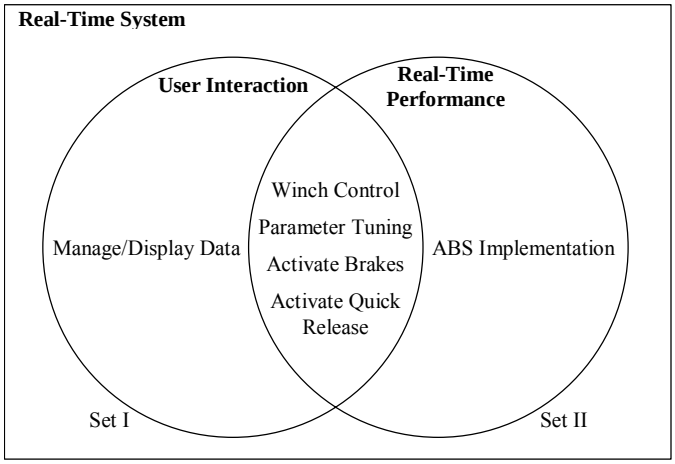

Figure 4.1 Real-Time System Functional Requirements Venn Diagram

User Interaction, Set I, defines those requirements that either require information from the user or give information to the user. Real-Time Performance, Set II, defines requirements that need to be accomplished within the specific real-time constraints assigned. The following figure defines the functional requirements.

Table 4.1 Functional Requirements' Descriptions

Functional Requirement	Description
Manage/Display Data	Convey/save information gathered during a experimental run to the user for immediate and future analysis
Winch Control	Allow the user to adjust the Winch's angular speed from the Host computer
Parameter Tuning	Allow the user to adjust the parameters governing the VI's
Activate Brakes	Allow the user to apply the brakes when desired during a run
Activate Quick Release	Release the cable at the start of a run
Implement ABS	Implement ABS braking when brakes are applied

Real-Time Constraints

Quantitative real-time constraints were defined to establish the level of programming effort needed. The following describes the method this was done.

Performance Categories

First, Set II of Figure 4.1 was divided between those functional requirements that needed to respond to the user in real-time and those that did not. The Venn Diagram, Figure 4.1, makes this identification as I $\cap$ II and II alone. As it turned out, only the Implement ABS requirement fell strictly under the need of heavy real-time performance.

Timing Needs

The timing needs for each category identified above, was established by determining the bottleneck or fastest response involved with each functional

requirement. The inverse of this response was then used to estimate the highest frequency the system could achieve. This would be the equivalent of the cut off frequency given by a bode plot of the system. Then, as directed by the Nyquist theorem which states that the sampling frequency required to capture the frequency of a signal must be at least twice the frequency of the signal, a frequency of at least twice that of the controlled system's maximum response frequency was chosen to determine the minimum real-time loop rate.(Van Doren)

For the first category, Real-Time Response to User, the bottleneck was established as the fastest time a human can respond to visual stimuli, as all the functional requirements included user input at the controls. Published data indicates that this response is no faster than 160ms. Hence, the update loop rate for reading in the users command and executing it would have to be, at most, 80ms or faster than 12.5 Hz.

The bottleneck for the second category required identification of the slowest controlled system response. The only functional requirement in this category was Implement ABS. As mentioned earlier, ABS works by activating and releasing the brakes to maintain the wheel slip about an operating point of maximum braking effort. The cycle includes measuring wheel speeds, calculating wheel slip, and activating the brakes accordingly. The bottleneck in this cycle is the response time of brake system or the highest frequency the brake system could oscillate. There was no experimental measurement for the time response of the brake system and so the simulation results were used. Since the time constant is generally used as good measurement of a first order system's response

performance and to establish a consistent method of determining real-time loop rate requirements, the time constant of the brake system was used to determine the maximum operating frequency of the brake system. According to the simulation, this value was 0.01s corresponding to a response frequency of approximately 100Hz. The Nyquist theorem hence requires a sampling rate of at least 200Hz to control the braking system. However, since it was desired to actually map amplitudes and profiles of the wheel and vehicle speeds a sampling rate of at least ten times the systems response was desired. Furthermore, since the intention of the laboratory was to help evaluate and tune vehicle-handling algorithms, a higher resolution would give more insight to the system's actual responses and timing issues. Therefore, the constraint for the real-time performance of the implemented ABS cycle was a loop rate less than or equal to 0.001s or a cycle frequency greater than or equal to 1000 Hz.

VI DESIGN

Algorithm

The functional requirements of the VI required, at the highest level, a loop that continuously ran until the user decided to quit the VI. The main loop would hence check the user inputs every loop and act accordingly. However, the two real-time performance categories could not be combined together at the same priorities as the wait periods introduced by the communicative functions crippled the performance required of the ABS. In order to solve this, a nested loop structure was used. The inner loop, fixed to iterate a specific number of times,

hosts the functions required to implement ABS. Outside the inner loop are all the communicative functions, with exception to the Activate Brakes signal from the remote control which was placed in the inner loop. Moreover, whilst the program was executing the inner loop, no communication is made with the host PC hence optimizing the real-time performance of the RT engine.

Once this nested loop strategy was identified, the following base algorithm was implemented.

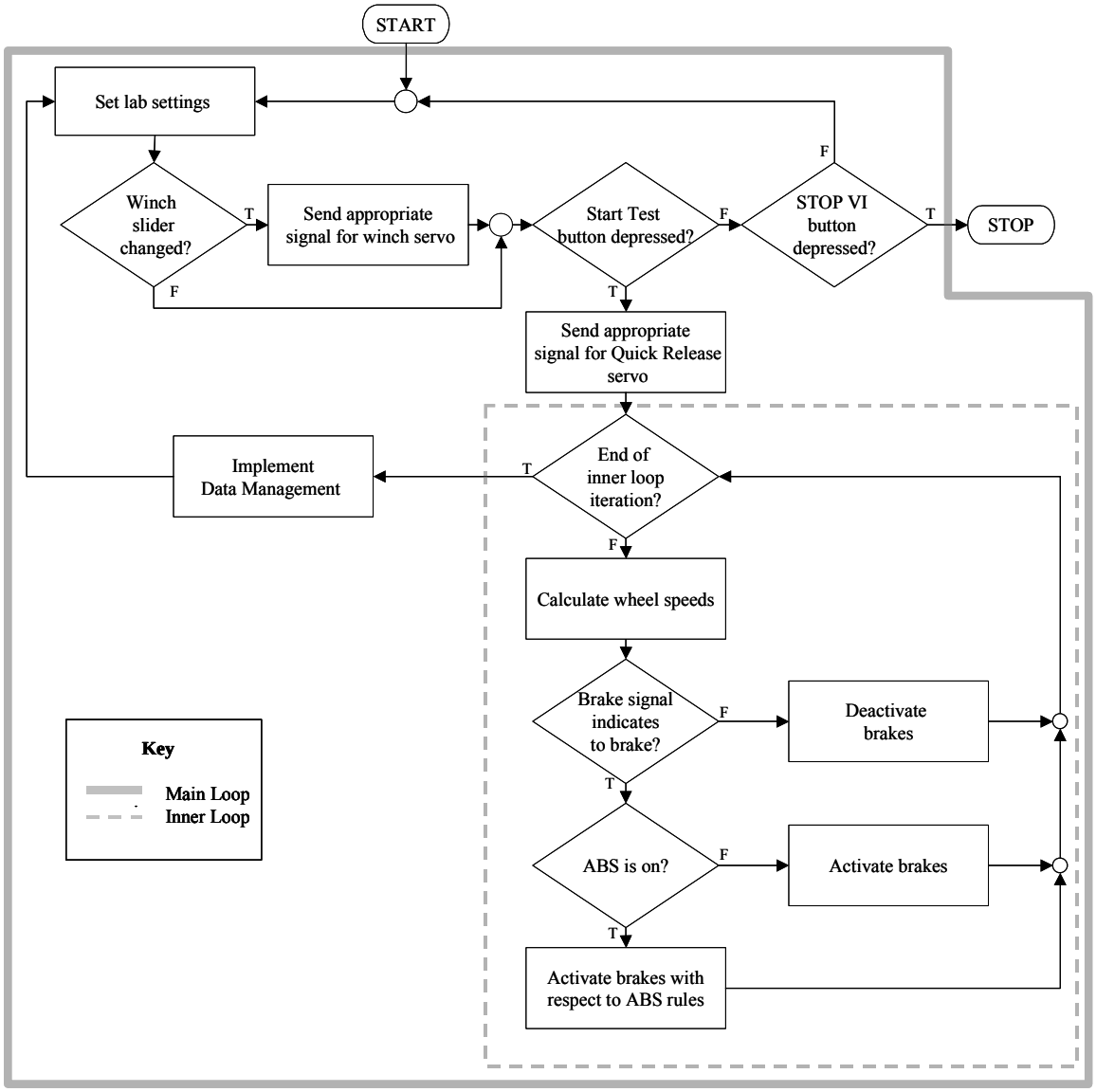

Figure 4.2 Basic VI Algorithm

The dynamics of the algorithm dictate that while in the Main loop the Winch speed can be controlled to bring the vehicle to a desired position on the ramp, and when desired, a Start Run button can be depressed to activate the Quick Release

and enter the inner loop. At this point, the car has just been released from the cable and the test run has started. If the signal to brake is activated, by using the trigger of the remote or by a timer, the brakes are applied to bring the vehicle to a stop. Upon completion of the loop, data logged during the run is displayed and the outer loop cycle begins again. The above cycle continues until the user depresses a Stop VI button, which causes the VI to exit the main loop and stop the program.

Function Specifics

For the different performance categories different data acquistion techniques were implemented. The following briefly describes the detailed level of programming needed to meet the real-time constraints.

Winch/Quick Release Control

The Winch and Quick Release Controls were reasonably easy to accomplish due to the relatively slow human response. Since both the Winch and Quick Release Mechanism were controlled by servos, the control method was similar for both. Using an already available function in LabVIEW RT, named Generate Pulse Train, a Winch Control VI was built by attaching a Slider type control to the duty cycle input of the Generate Pulse Train function. Since the Slider control is accessible from the Panel the duty cycle of the signal going to the Winch servo could be changed while the VI was running, hence control of the Winch speed was achieved.

The Quick Release Mechanism servo only required two positions for the Locked and Release positions and therefore a Button type control was used to switch the duty cycle from one setting to the other. A mechanical return type

button was chosen, from the list of options, to reset itself to the false position once released. This action guarantees that the Quick Release mechanism remains locked unless the button is depressed.

It should be noted that the Generate Pulse Train VI is a high level function that incorporates sub functions to configure counters on the DAC to generate the pulse train and, in doing so, these sub functions are executed every time the counter is called costing valuable processing time.

Implement ABS/Activate Brake

The implementation of ABS required acquisition of encoder frequencies, the pulse width of the Activate Brake signal, and generation of analogue signal for the right and left brakes according to the rules of the ABS algorithm used.

At first, the implementation of acquiring the encoder frequencies was done using higher levels VIs found available in the data acquisition library that came with LabVIEW. These VIs function by sampling the counter data for a certain period and giving an output value, which corresponds to either the "frequency of the pulse", or "pulse width of the pulse" whichever the case selected of the VI. The sampling period is either set by specifying the "gate width" for frequency measurement and/or specifying the wait period using Wait VIs inside these, high level, VIs. The loop rate was the sum of the time taken for executing all these VIs. Initially the control loop was running on the order of 200 ms as the "Measure Pulse Width VI" took a relatively long sampling time to acquire the pulse width of the Activate Brake signal. This was reduced to about 40-50 ms range when the sampling period (wait time) was reduced, and was the fastest loop time achieved

using these high level VIs. The advantages to using these "high level" VIs were their ease of use. However, they carried routines, such as Configure Counter VIs, that were unnecessarily executed every iteration, costing valuable time.

The next step was to reduce the time to acquire the encoder frequencies by using lower level VIs. Though more difficult to use, the lower level VIs allowed specific programming of the counter timer hardware and made it possible to extract only the necessary functions for use in the inner loop. A scheme was set to program the hardware to store, into a buffer in memory, the number of clocks of an internal time base for the duration of the high pulse generated by a TTL incoming signal. This scheme took advantage of the Direct Memory Access (DMA) functionality of the board, which allows for the board to put measurements directly into the computers memory without using the computers processor, hence no overhead is added to chores of the CPU. The buffer was then read at each iteration of the inner loop and the actual pulse width in seconds was determined by dividing the number of counts by the internal time base frequency. This method achieved inner loop rates of less than 1ms and allowed the same VIs to measure the frequency of the encoder signals and pulse width of the Activate Brake signal, since both are TTL signals.

As indicated by the application algorithm, once the signal to activate the brakes was given and the speed of the wheels determined an appropriate voltage was generated to drive each of the Brake Motors. Since each experiment was run for the case of an extreme stop, only two voltage levels were needed – one for full brakes and the second for no brakes. A high level VI that came with LabVIEW

called Single Update was used to generate the voltages. Since this function only configured the hardware on the first iteration of the real-time loop it was efficient enough to meet the real time specifications set for the control algorithm.

User Interface

The User Interface (UI) was designed such that analysis, saving, and recalling of data could be made as well as controlling the experimental setup and procedure. The figure bellow shows the general layout of the user interface.

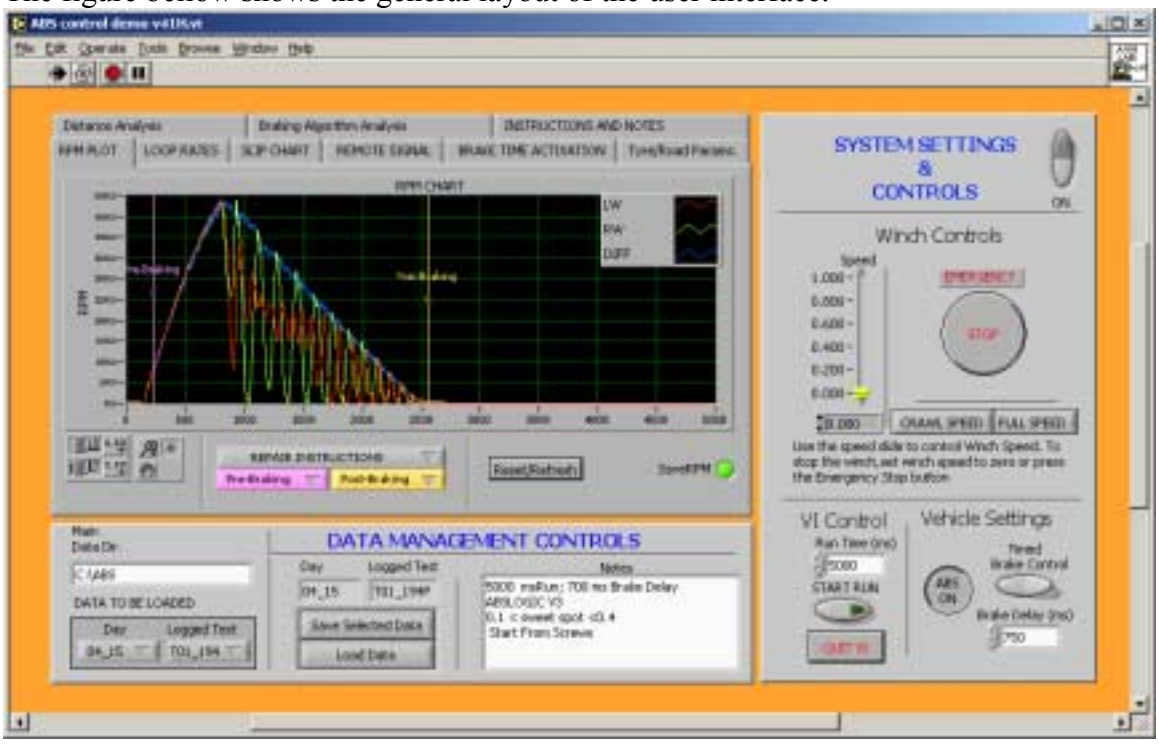

Figure 4.3 VI User Interface

The UI was written to run on the host (windows) PC and communicates with a Real-Time engine VI through TCP/IP, a general network protocol, and VI server, a proprietary technology of National Instruments. This way the UI VI could utilize the host PCs processor for data management and analysis whilst still allowing the user to control the real-time functions on the RT engine.

The UI is divided into three sections, a lab control section, a data management section, and a data viewing section. The UI was designed to allow new users to quickly use the lab with minimum experience and training. The three sections of the UI are briefly described bellow.

UI Details

The section labeled System Settings and Controls allows the user to control the winch used to pull up the vehicle, set the parameters for each run, such as using ABS or not, and finally start a Run. The Run Time parameters sets the amount of time the inner loop, i.e. the braked vehicle run. The Timed Brake Control switch can be toggled to Remote Brake Control to allow the user to choose a computer initiated braking or a manual initiated braking by a person using the radio control. If the switch is set to Timed Brake Control, then the Brake Delay parameter must be set to set the time delay before braking is initiated. It should be noted that the Run Time and the Brake Delay parameters represent the number of iterations of the real-time inner loop and are not precisely milliseconds. The indication of milliseconds is labeled to give the user an intuitive feel. However, the values are still a good approximation of time as the real-time inner loop iterations were intended to run at 1ms loop rates as per the inner loop real-time requirements

described earlier. The Run Time is hence the number of loops the inner loops iterates for and the Timed Brake Control sets the iteration for the initiation of braking. Furthermore, with the Timed Brake Control, once initiation has begun, the vehicle is broken until the inner-loop iteration reaches the Run Time count. The data retrieved during a run can be saved and viewed in the other two sections described bellow.

The Data Management Controls section allows the user to save the data of a run and/or recall saved data from previous runs. To prevent runs from overwriting each other, a new folder is created every time a new run is saved. The folder is named according to the date and time so no two runs will have the same file name. Separate entities of data, such as the right wheel speed and left wheel speed, are stored as text files that are tab delimitated for ease of viewing in other software such as Excel and MatLab. Moreover, a 'notes' file is also saved so users can make notes unique to each run. When old data is recalled, the notes are then displayed accordingly.

Finally theDialogue Tab section allows various methods of viewing and manipulating recorded data displayed as graphs. Utilities, such as comparing two runs are included for fast analysis of comparative ABS algorithm schemes. Instructions on how to use the laboratory and VI are also included as one of the Tabs.

ADDITIONAL FEATURES

Some additional features were included for experiment control and parameter setup. The extra feature for the experiment control was the inclusion of

automatically triggering the brakes after a user-defined period. This allows the repeatability of each run as the brakes can be applied precisely at the same time from run to run.

There is also a feature that allows the user to manipulate a μ-λ curve graphically. This feature does not benefit the lab setup, as intended for this thesis, but was included for future experiments where detailed Tire-Road information is needed.

Chapter 5: Experiments and Results

EXPERIMENT SETUP

The completed lab combined all of the components mentioned in chapter 2. The vehicle was instrumented to acquire the wheel and vehicle speeds and had independent cable actuated front disk brakes, powered by modified Futaba servos, driven by amplified brake signals from the RT Engine. The RT Engine was programmed using LabVIEW RT and ran a VI that controlled the Winch, implemented the braking algorithm, and transmitted data back to the Host PC. The Host PC ran the User Interface VI, allowing the user to control the Winch, set

lab control parameters, and view and manage the data received from the RT Engine.

The experiments run were designed to evaluate the potential of the Controls Vehicle Laboratory (CVL) via straight ABS braking tests. The goal of the first experiment was to record the performance of the vehicle without any improvements to the ABS algorithm, used in the simulation. The results of this test would indicate the accuracy of the simulation and the ability of the vehicle stop in a shorter distance with ABS than without ABS. The second experiment tested the labs capability in providing enough data to fine tune the braking algorithm and hence improve the ABS braking performance. The second experiment was simply a replication of the first experiment but with the ABS algorithm tuned according to the data given from the first experiment. The importance of this experiment is the evaluation the lab's ability on improving AVH algorithms once implemented on real systems. The second test is therefore representative of the procedures taken by manufactures in fine-tuning ABS systems for life size vehicles.

Experiment Procedure

Though CVL was designed to provide a flexible platform for various ABS and future AVH evaluations, it was necessary to perform systematic runs to ensure repeatability and comparable results. To ensure this only a few conditions had to be met and are listed as follows:

Onset of Braking Vehicle Velocity: The initial velocity upon braking had to remain constant so distance relations could be compared. This was accomplished by winching the vehicle up the ramp to a pre-marked position that would be used for all tests. Furthermore, a computer controlled timed braking was set to be equivalent from run to run. This would ensure that the computer would initiate braking at exactly the same time from the release of the vehicle.

Tire Road Parameters: To ensure that the tire-road parameters remained fairly constant, the tire and road surface were wiped clean before each run.

Run Path: The vehicle was set to follow the same straight path for each run as to reduce the amount of side forces effecting the braking distance.

Once these conditions could be ensured the vehicle was brought to a marked starting position approximately 1.8m up the ramp, the wheels were straightened and the Start Run button was depressed on the UI on the Host PC. The car was automatically released and the vehicle started braking after the desired delay was reached. The Run Time of each test was set to 5 seconds, which was purposely set to be longer than the time the car took to come to a complete stop to ensure that no data would be missed. The UI was then populated with the results, notes were entered to describe the run and the data was saved. This same procedure was followed for each run implemented.

RESULTS

For each run there were six data files produces. The following table describes the file names and the data contained.

Table 5.1 File Names of Data Saved with Description and Format

Data File	**Description and Format**
BRACT	Signal representing that the braking has occurred. Integer format. 0 : Signal to Brake has not been sent 1: Signal to Brake has been sent.
BRKSG	Brake signal sent to each brake servo. Integer format. 0 : Brakes Off 1 : Brakes On
LOOPR	Recorded loop rates in milliseconds for each loop iteration. Decimal format.
RPM	2-D Array of recorded RPM for the front wheels and equivalent vehicle speed (from differential) in RPM. Decimal format. Row number indicates the loop iteration. Column One : Left Wheel RPM. Column Two : Right Wheel RPM Column Three : Differential RPM/Equivalent Gear ratio.
SLPCH	2-D Array of calculated wheel slip for each loop iteration in decimal representation from 0 to 1. Integer format. Rows number indicates the loop iteration Column One : Left wheel slip Column Two : Right wheel slip
TIME	Time stamp for each loop iteration. Decimal format.

First Experiment Results – General Lab and ABS Evaluation

The first experiment was run several times with data being recorded for each run. The results for the Loop Rates, ABS Performance, and comparisons between locked-wheel and ABS controlled braking are shown bellow with respective comments on each.

Loop Rates

Figure 5.1, bellow, shows the typical loop rate performance for a Run with ABS using the original ABS braking algorithm as used in the simulation. The plot describes the time in milliseconds for each iteration of the loop. The on board CPU clock of Real-Time Engine was used to time each loop. This method was made possible with the help of VIs available at the National Instruments web site which directly count the CPU's clock edges to determine the loop rate. The Real-Time Engines CPU was a Pentium III 333MHZ. Since the VIs simply counted the number of clock edges between loops, the resolution of each loop reading can be taken as the inverse of 333MHZ or 3.003 nanoseconds. Figure 5.1 indicates that the loop rates fluctuated between 0.95 ms and 1.2 ms with a mean of 1.02ms. The indeterminism can be attributed to the error checking and control evaluations made in the real-time inner loop to determine the decision to apply the brakes fully or not. This is easily validated by comparing the loop rates to a plot of the loop rates for the same Run parameters except with the ABS turned off, i.e. Locked-wheel braking, as shown in Figure 5.2. The non-ABS run reveals a similar profile as the ABS run but with a 0.15 ms overall decrease in loop rates which strongly hints that the ABS logic must attribute for 0.15 ms and that the rest of the processing time comes from wheel speed readings and sending voltage signals by. Subtracting the loop rates for non-ABS from the loop rates of the ABS run shows relatively uniform difference of 0.15ms. . Figure 5.3 shows a graphical representation of this operation.

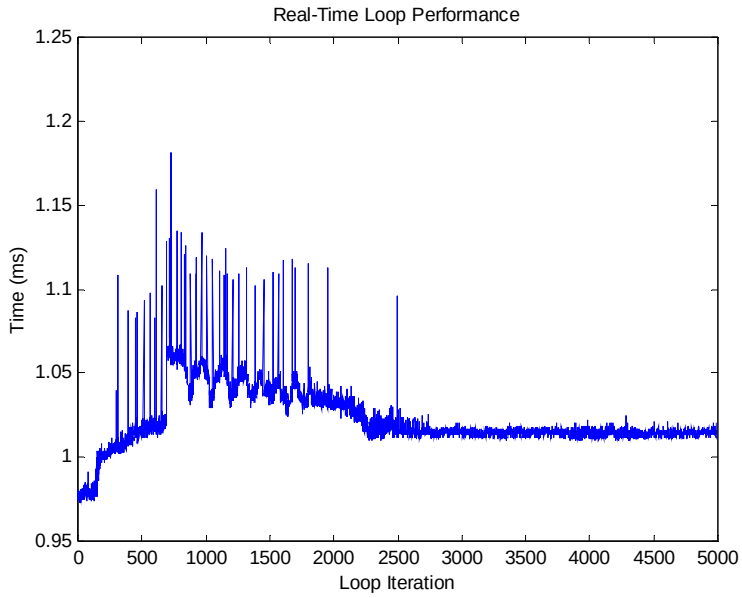

Figure 5.1. Real-Time Performance for Run 4_14\T09_135P: ABS -ON

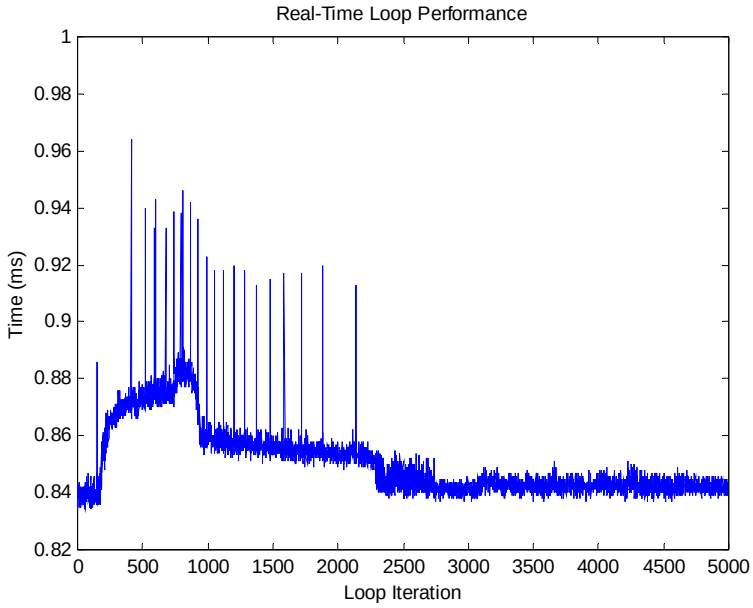

Figure 5.2 Real-Time Performance for Run 04_14\F09_165P: ABS -OFF

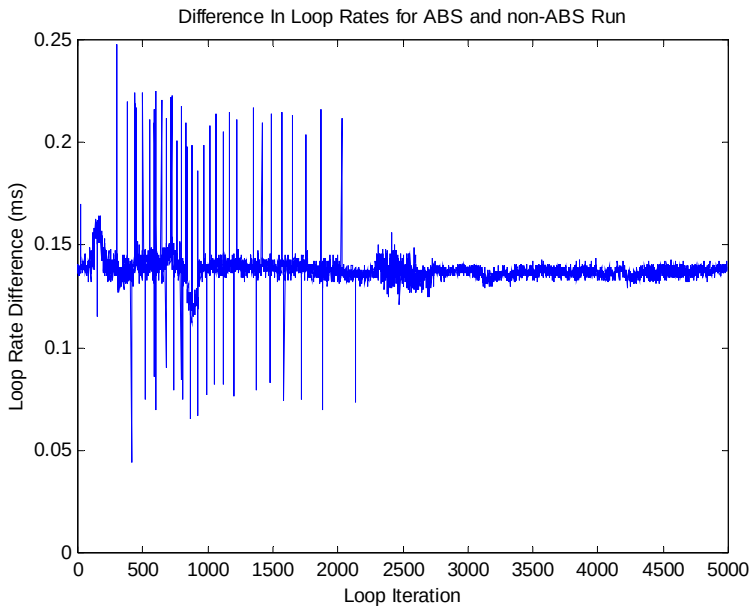

Figure 5.3 Loop Rate Difference for ABS Run and non-ABS Run

ABS Performance

The ABS performance was primarily evaluated by viewing the wheels and differential speeds. Ideally the wheel should not completely lock up nor spin at the equivalent vehicle speed as shown in the simulation. This was not the case with the actual runs using and the results showed that the wheels underwent complete lock-up and spin. Figure 5.4 shows the RPM data recorded for Run 4_14/ T09_135P.

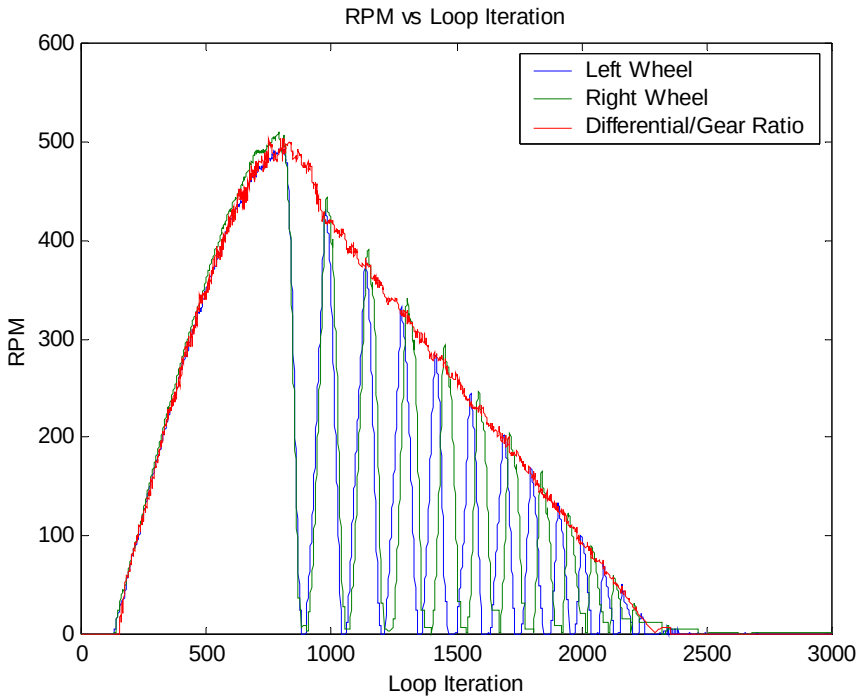

Figure 5.4 RPM Readings for Run 4_14/ T09_135P

The wheel slips were also evaluated to determine the performance of the ABS brake stop. Figure shows that the wheels slip for each wheel traveled from 0 to 100%. The data before the release of the vehicle is resultant of using a very low vehicle speed (near zero) to calculate the speed. This section of data can therefore be dubbed erroneous and is not consistent from run to run. However, once the vehicle moved, the slip calculation became accurate as there were well-defined signals representing speeds from the encoders. The bad data could have been easily filtered out with a conditional statement. This was not desired, as the extra code would have negatively affected the control loop rates, since execution time for the code overhead would also increase. Furthermore, the objective of the

slip data was to view the performance during braking, which, as the figure shows, recorded well.

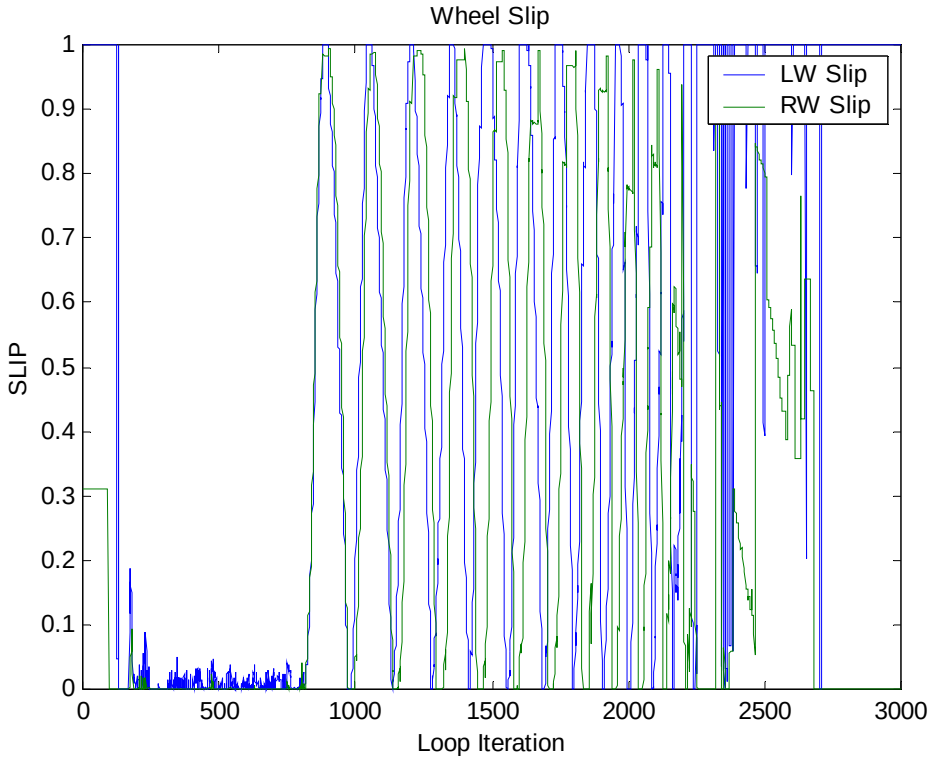

Figure 5.5 Wheel Slip for Run 4_14/ T09_135P

Braking Distances

Comparisons between the ABS and non-ABS stops revealed little to no improvement with ABS over locked-wheel stops. The Figure 5.6, bellow, the

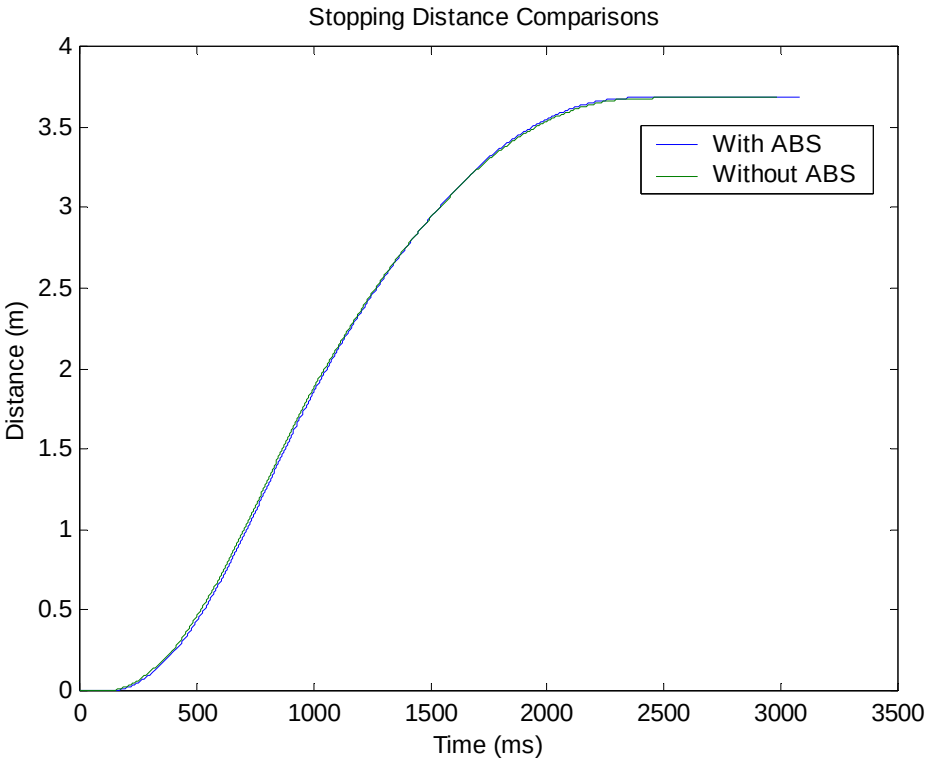

Figure 5.6 Distance Comparison Between Stops With and With-Out ABS

Second Experiment Results – Tuned ABS Algorithm

ABS Tuning

Selectively displaying data from the first experiment, using the Braking Algorithm Analysis tool, allowed for visual determination on the response the braking system had to the signal given for activated and deactivated the brakes. Figure 5.7 shows the UI with the Braking Algorithm Analysis tool selected. The data displayed in the figure is from Run 4_14/ T09_135P. Using magnifying tools

provided by the UI, the graph was zoomed in to get a clearly idea on exactly how the left wheel was responding to the Brake Signal. From this, it was determined that the braking system had longer response than was simulated, allowing the wheel to fully lock up.

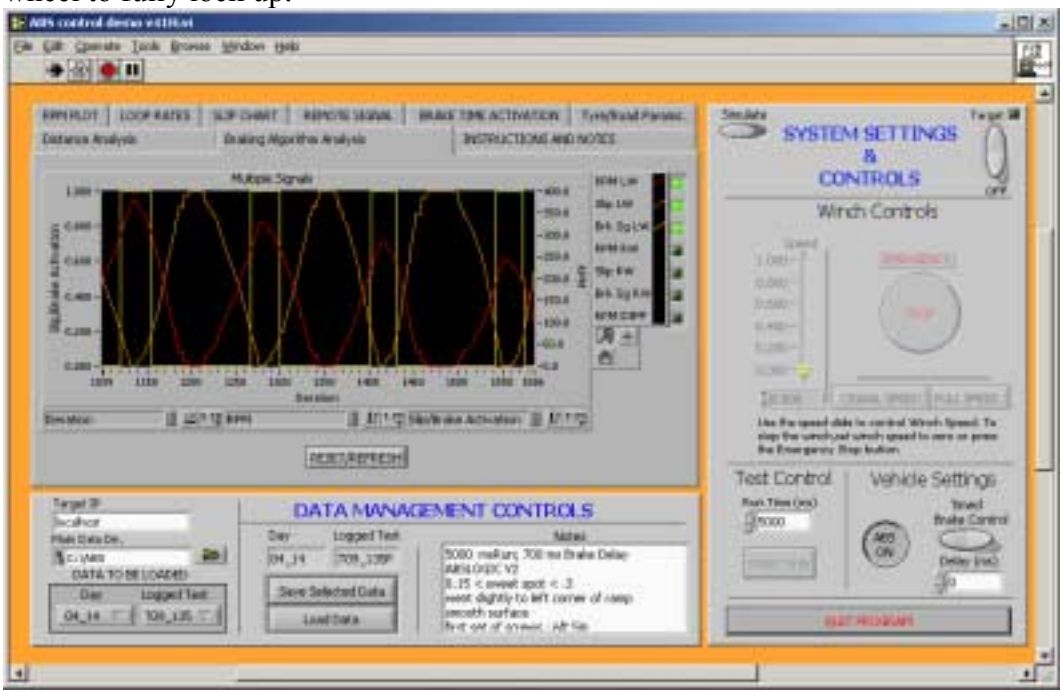

Figure 5.7 UI Braking Algorithm Analysis Tool (Left-Wheel Data Displayed)

A decision was made to counteract the slow response by sending the signals to activate and deactivate brakes at earlier times. Therefore the ABS algorithm was modified to be as shown in Figure 5.8. The ABS was also tuned to have a much narrower sweet spot where λ_{low} and λ_{high} were changed to 4% and 10.5 %. These numbers were estimated purely based on the visual analysis of the data shown using the UI Analyze ABS Algorithm tool, and the learned knowledge that the wheel must be locking up due to a delayed response in releasing the brakes i.e. the

sweet spot region must lie to the left of what was estimated in chapter 2. In essence the ABS algorithm was tuned to increase the actual performance.

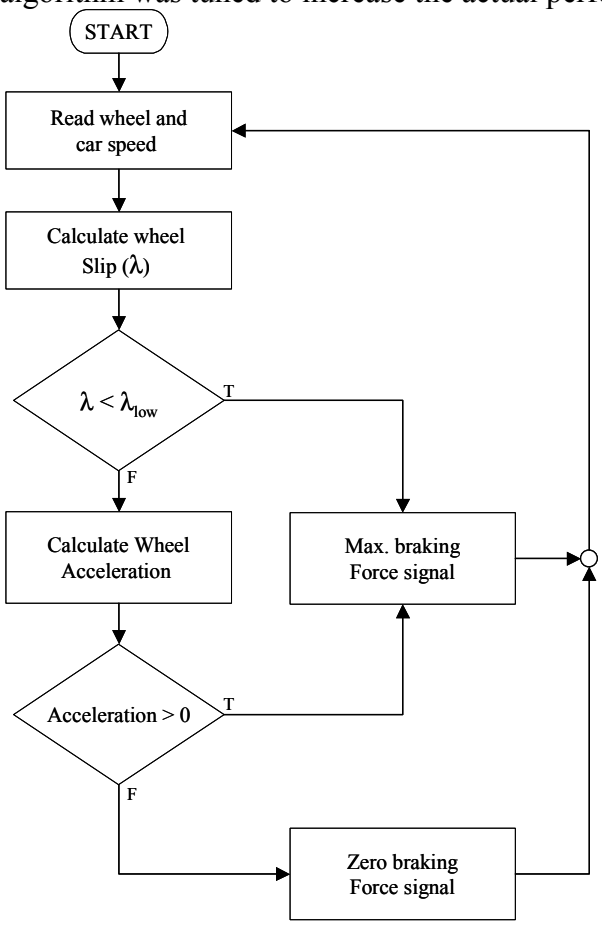

Figure 5.8 Tuned ABS Algorithm for Second Experiment

ABS Performance

An improvement of ABS performance was witnessed after implementing the new ABS algorithm. However, the improvement was not so for both front wheels. The RPM data, shown in for the wheels shows that the left wheel reached more of an ideal performance than the right wheel, as its RPM resisted full lock-up and full

spin upon initial braking. Upon braking, the right wheel did avoid lock-up but then continued as before.

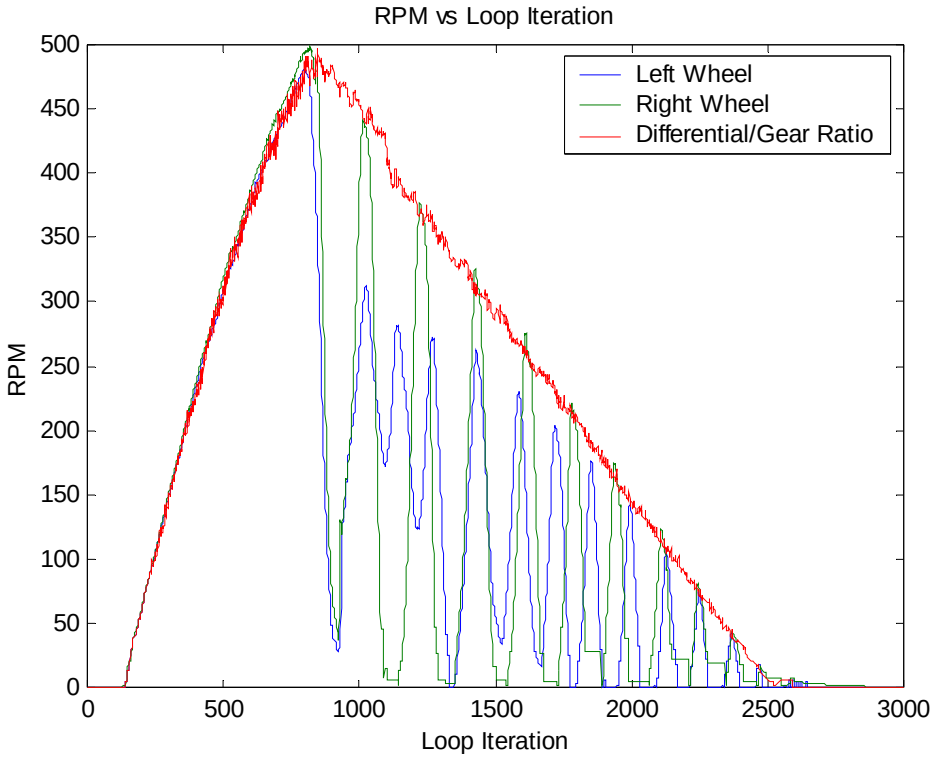

Figure 5.9 RPM Plot of Run with Improved ABS Algorithm

The plots for the wheel slips also indicated an improvement as the left wheel clearly avoided 0 or 100% wheel slip for the majority of the braking process. Furthermore the behavior of the wheel slips more closely matches that of the simulated run. Again, this was more apparent for the left wheel.

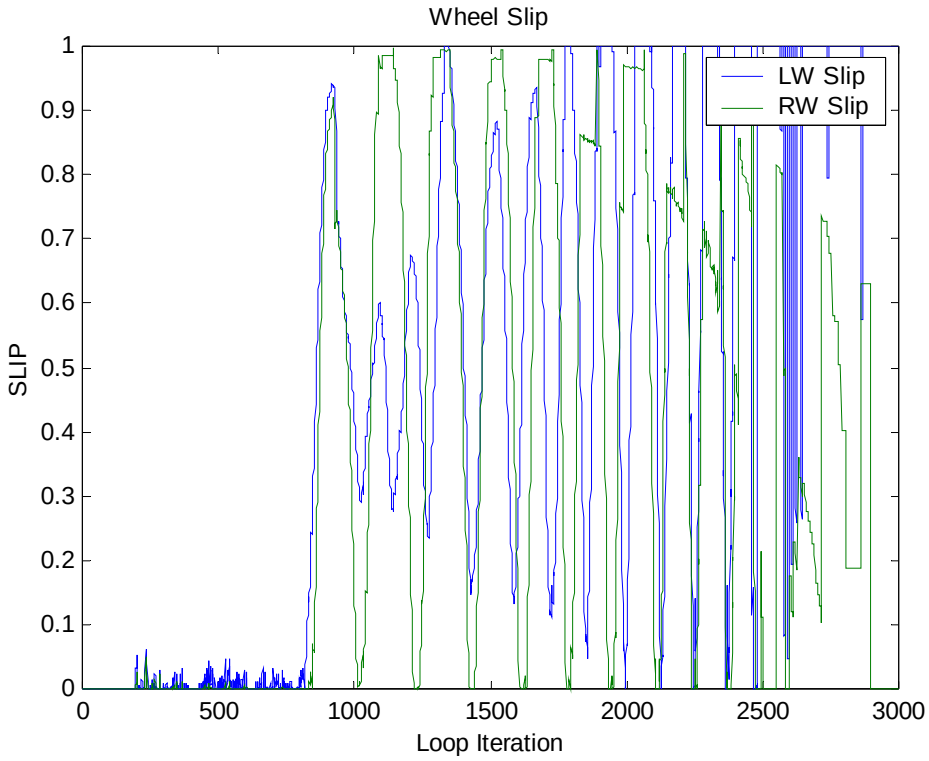

Figure 5.10 Wheel Slip for ABS Stop with Improved ABS Algorithm

Braking Distances

When braking distances were compared for stop with and without ABS implemented, the results showed improvement for the ABS stops which is consistent with RPM and Wheel Slip results. When plotted against a run where the stop was implemented with fully locked brakes, the stops with ABS distinct and consistent shorter braking distances. The compared distances for Run 4_23/ T02_125P, shown in Figure 5.11 bellow.

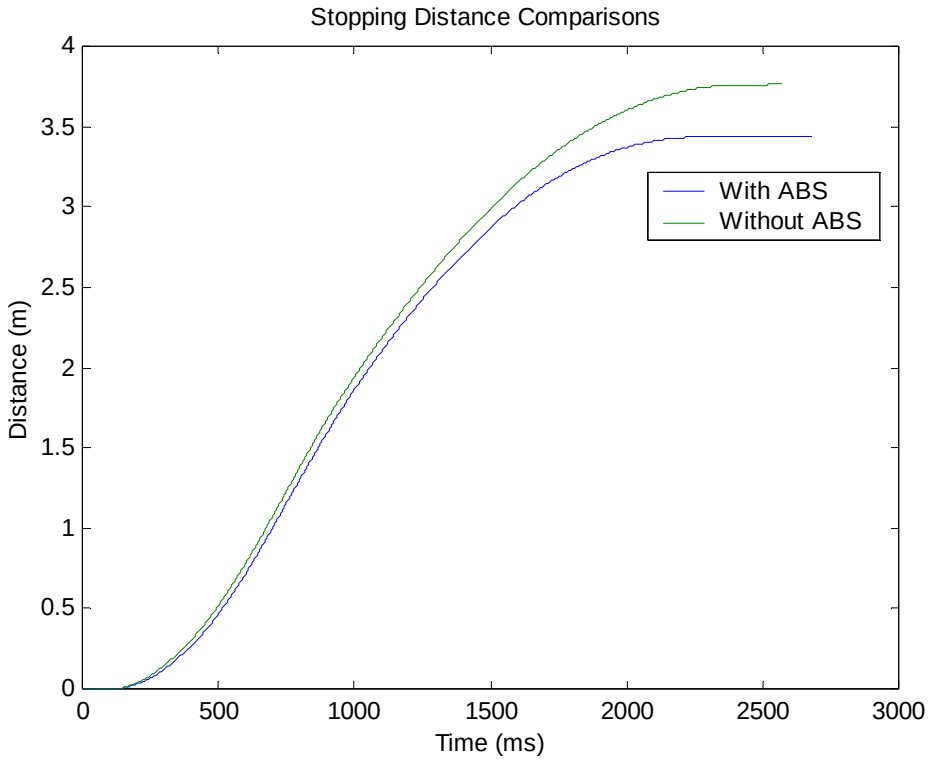

Figure 5.11 Stopping Distance Comparisons for Improved ABS Algorithm

Chapter 6: Conclusion and Recommendation for Future Work

SCALED ABS BRAKING

The objective of this thesis has been met. A scaled vehicle has been fitted with ABS and a laboratory has been built to test ABS braking algorithms. Testing has been done to evaluate the laboratory as a testing tool for ABS algorithms applied to a scaled vehicle. Furthermore, experiments show that the $1/5^{th}$ scale vehicle can be used to demonstrate the differences between locked wheel braking and ABS controlled braking. It has also been verified that a PC based controller is capable of implementing control algorithms within the real-time requirements of the ABS system.

FUTURE WORK

Further work is necessary to realize the full potential of VCL to be used as an AVH laboratory. It has been shown and verified that the implementation of ABS on $1/5^{th}$ scale car can be implemented. This opens the door to the possibilities of implementing more advanced systems by building upon such a laboratory. The foundation has been laid and tested to show one possible laboratory setup for the study of active vehicle systems for handling purposes. The following recommendations are suggested for improvement of the setup:

Braking System

Though the results show that the current braking system is adequate to demonstrate differences between ABS and locked-wheel stops, it must be

improved to increase the lab's sensitivity to ABS algorithms. The physical design of the disc and brake caliper system introduces play as the disc must travel longitudinally to stop against the outer (stationary) brake pad before any significant normal force can be applied from the inner (moving) brake pad. This motion introduces both a dead zone and stiction, due to the sloping of the disc as it pivots at the center before sliding. This action drastically slows the braking response and is clearly evident through comparison of the Wheel Slip plots made by the simulation and those of the actual tests. Furthermore, the performance of this "floating disc" design was found to be very sensitive to the distance between the brake pads while the system was at rest, hence making tuning of the physical brake system tedious and difficult. The optimum design of the brake system was not a focus of this thesis but an improvement must be made before any critical evaluations of ABS algorithms can be made.

It is also highly recommended that ABS brakes be designed and installed for the rear of the vehicle. In order for VCL to meet its full potential, the test vehicle should realistically simulate a commercial vehicle. Though there are numerous scaling issues that need to be studied, the $1/5^{th}$ scale vehicle should have a complete braking system for all wheels. Introducing rear wheel braking will complete the vehicle part of the laboratory in its conquest of replicating the true challenges faced by vehicle control system designers, such as the classical problem of vehicle speed estimation.

Other Areas of Study

It is this author's view that the lab created has great potential for economic and feasible research and instruction in vehicle systems as well as study in other classical fields of engineering such as design and experimentation. The laboratory designed and built spans many areas of engineering, from design to controls to materials. The advance of computers and their accompanying software has allowed engineers to assimilate the power of intelligent systems and implement them in their design. The drive has always been toward creating newer, better, faster and cheaper solutions than those that exist today. The hope is that this laboratory will further facilitate that drive, accelerate ideas such as independent steering, and contribute to the laboratory tested and verified phase of a technology's life span.

CONCLUSION

By no means is VCL complete. The idea is that a lab can be created with enough flexibility to allow for researchers and instructors implement and teach new ideas and basic principles. The result of this thesis is that a laboratory that incorporates a $1/5^{th}$ scale vehicle with front brakes and an accompanying ramp and track, controlled by a graphical user interface as the seed for the foundation of an on going drive for the study of Active Vehicle Handling.

Appendix A. Vehicle Component Drawings

Appendix B. Simulink Diagrams for Simulation

Below are figures of the Simulink block diagrams used for simulation of the 1/5th scale vehicle undergoing braking.

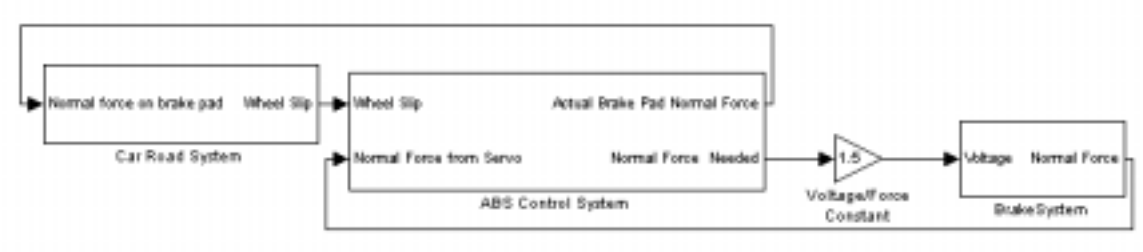

Figure B.1 Main System Block

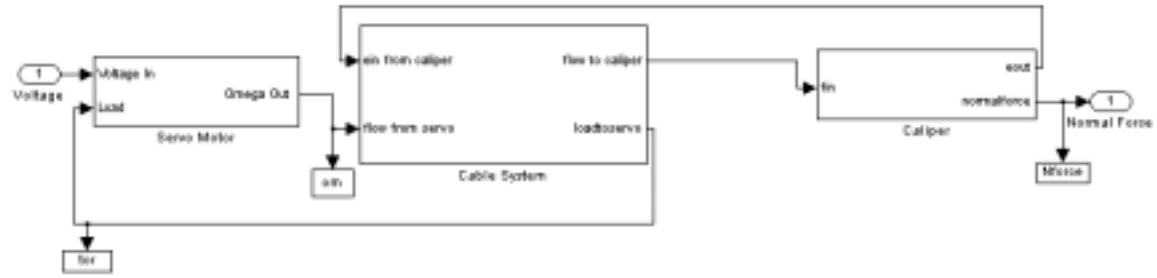

Figure B.2 Brake System Main Block

The Simulink model bellow, representing the brake servo, was created to closely represent a Bondgraph and follows the same concepts. The blocks representing the elements were given to the author by a colleague named Dwight Landen.

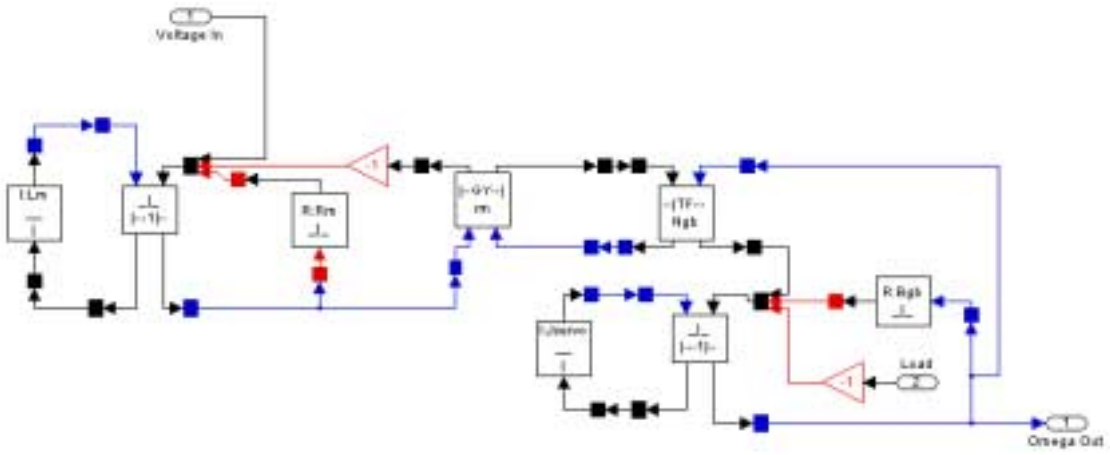

Figure B.3 Brake Servo Block

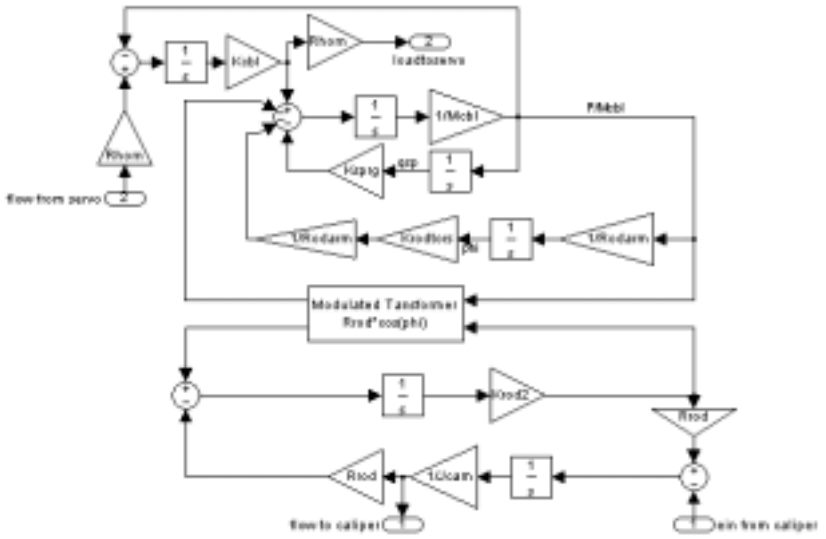

Figure B.4 Cable System Block

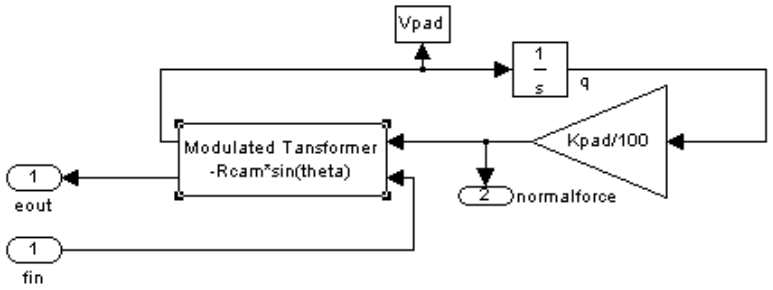

Figure B.5 Caliper Block

CAR ROAD SYSTEM SIMULINK BLOCKS

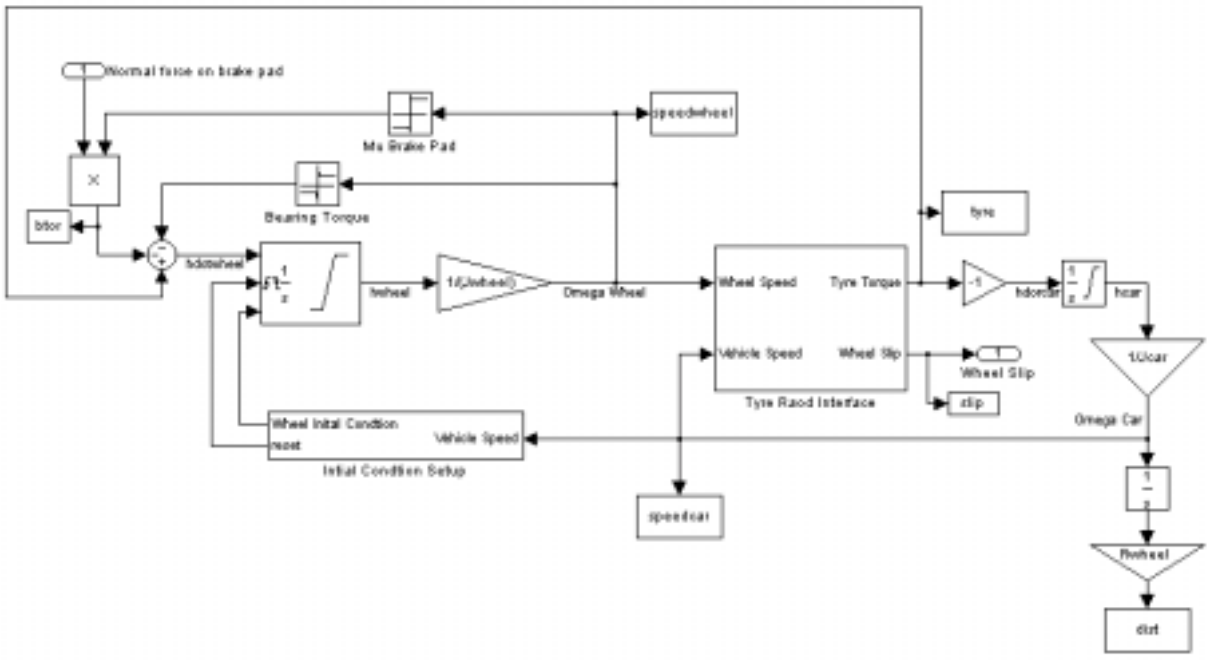

Figure B.6 Car Road System Main Block

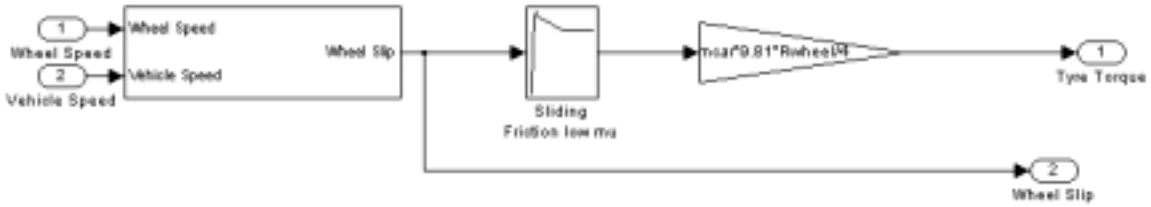

Figure B.7 Tyre-Road Interface Block

ABS CONTROL SYSTEM BLOCKS

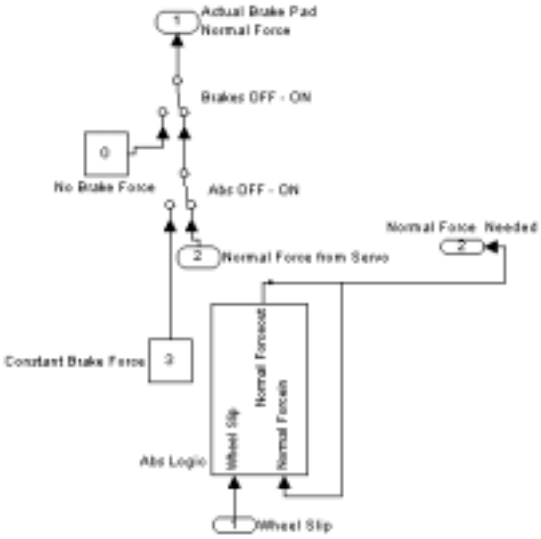

Figure B.8 ABS Control System Main Block

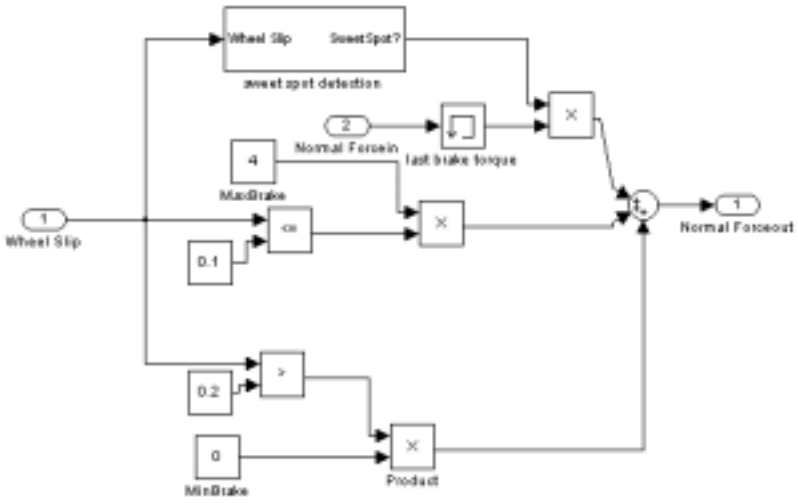

Figure B.9 ABS Logic Block

References

1. Ulsoy, A.G., Peng, H., Vehicle Control Systems – Lecture Notes, "Chapter 8 Traction Control", M E 568 1997

2. French, T, *Tire Technology*. Bristol and New York: Adam Hilger, 1989

3. Gillespie, T. D. *Fundamentals of Vehicle Dynamics* Warrendale, PA: Society of Automotive Engineers, 1992

4. Wong, J.Y. *Theory of Ground Vehicles*. New York, NY: John Wiley & Sons, Inc. 1993

5. French, T, "Construction and Behaviour Characteristics of Tyres," *Proc. Of the Institution of Mechanical Engineers, Automobile Division*, AD 14/59, 1959

6. Automotive 101, autoshop-online.com. "Brake Systems," August, 2000. http://www.autoshop-online.com/auto101/abs.html

7. Khatun, P. Bingham, C.M., and Mellor, P. H. "Comparison of Control Methods for Electric Vehicle Antilock Braking/traction Control Systems," *Brake technology, ABS/TCS, and controlled suspensions*, Warrendale, PA : Society of Automotive Engineers, March 2001.

8. *Vehicle Dynamics Terminology*, SAE J670e, Society of Automotive Engineers, 1978

9. Wellstead, P.E. "Analysis and redesign of an antilock brake system controller," *IEEE Proc. – Control Theroy Appl.,* Vol. 144, No. 5, September 1997, pp. 413 – 426.

10. Rosenberg, R., Karnopp, D., *Introduction to Physical System Dynamics*. New York, McGraw-Hill Inc. 1983

11. Juvinall, R., Marsheck, K., *Fundamentals of Machine Component Design, Second Edition*, New York, John Wiley & Sons, Inc.1983

12. Kachroo, P., Smith, K., "Experimental Setup and Testing for Verification of Similarity between Road-tire Interaction Characteristics of Scaled Models and Full Scale Vehicles," SPIE VOL 3207, 1998, pp. 306 – 316.

13. Anthony, B. Will, Stanislaw, H. Zak, “Antilock brake system modeling and fuzzy control,” International Journal of Vehicle Design, v24, n1, 2000, Inderscience Enterprises Ltd, Geneve-15, Switzerland, p 1-18

14. Jun, Li, Jianwu, Zhang, and Fan, Yu, “An Investigation into Fuzzy Control for Anti-Lock Braking System Based on Road Autonomous Identification,” *Brake technology, ABS/TCS, and controlled suspensions*, Warrendale, PA : Society of Automotive Engineers, March 2001.

15. Athan, Timithy War, Papalambros, Panos Y., “Multicriteria Optimization of Anti-Lock Braking System Control Algorithms,” Engineering Optimization, v 27, n 3, 1996, Gordon & Breach Science Publ Inc, Newark, NJ, USA, p 199-227

16. Agilent Technologies

17. Lawrence, Peter D., Mauch, Konrad, *Real-Time Microcomputer System Design: An Introduction*, McGraw-Hill, Inc New York, NY, 1987